

CHEMISTRY

A **European** Journal

Supporting Information

Enhancing Potency and Selectivity of a DC-SIGN Glycomimetic Ligand by Fragment-Based Design: Structural Basis

Laura Medve^{+, [a]} Silvia Achilli^{+, [b]} Joan Guzman-Caldentey^{+, [c]} Michel Thépaut,^[b]
Luca Senaldi,^[a] Aline Le Roy,^[b] Sara Sattin,^[a] Christine Ebel,^[b] Corinne Vivès,^[b]
Sonsoles Martin-Santamaria,^{*, [c]} Anna Bernardi,^{*, [a]} and Franck Fieschi^{*, [b]}

chem_201903391_sm_miscellaneous_information.pdf

Table of Contents

Table of Contents	2
Results and Discussion	3
Docking of the designed ligands	3
MD Simulation of the DC-SIGN/ 16 complex.....	5
SPR Competition assay: inhibition data	6
Biophysical characterization of 16 binding to DC-SIGN	7
Structural analysis	8
Experimental Procedures	9
Computational methods	9
Synthesis.....	10
Alkynes used in CuAAC reactions and corresponding triazole derivatives	11
Synthesis of 16 (Scheme S1).....	11
Compound characterization	12
References.....	18

Results and Discussion

Docking of the designed ligands

Compounds shown in Figures 3 and S1 were docked in three different 3D structures of DC-SIGN. Two structures corresponded to two of the available crystallographic structures of DC-SIGN (PDB IDs 2XR5 and 2IT5), and the third structure corresponded to the average structure from the MD simulation of apo DC-SIGN from PDB 2XR5 (2XR5-MD).

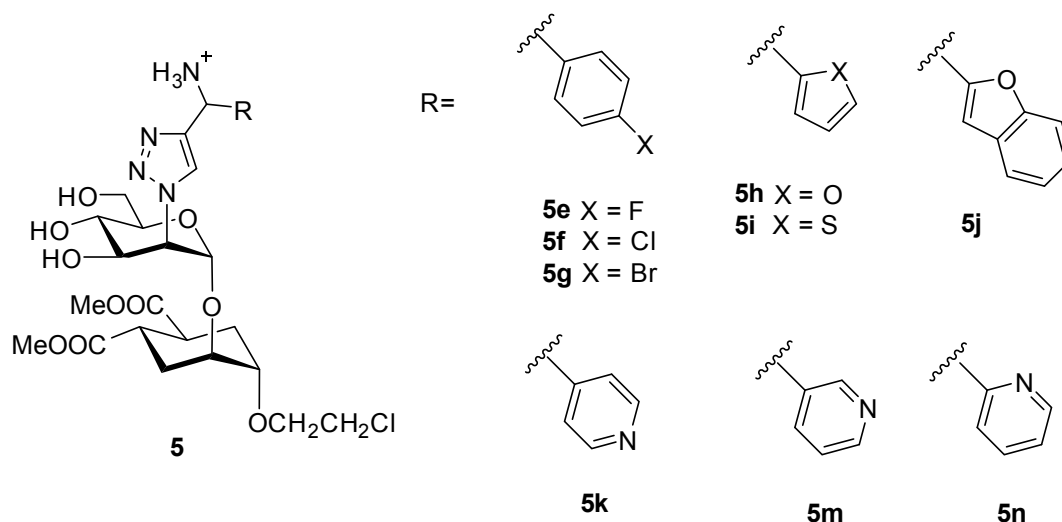


Figure S1. Triazole derivatives designed as DC-SIGN ligands together with compounds from Figure 3. For each ligand, *R* and *S* stereoisomers were calculated.

Although there are no major differences between the two X-ray crystal structures (2FXR5 and 2IT5), subtle changes in some amino acid side chains can be found in the carbohydrate binding region. In particular, the Lys368 side chain, which is exposed to the solvent in PDB 2XR5, is oriented towards the bound ligand in PDB 2IT5 (Figure S2). This different orientation could lead to changes in the docked pose and in the predicted binding energy. Additionally, the Val351 side chain is very close to the carbohydrate binding site in PDB 2XR5 and two different conformations (A and B) are observed. In order to explore this variability, we performed MD simulations of the apo DC-SIGN protein from PDB 2XR5 of both 3D structures corresponding to the two Val351 rotamers (A and B). We observed that rotamer B was more stable along the simulation. A widening of the ammonium binding pocket was also observed during the simulation, mainly due to the displacement of the Phe313 side chain. The average structure of the MD simulation from rotamer B (2XR5-MD) was the one further used for the docking studies.

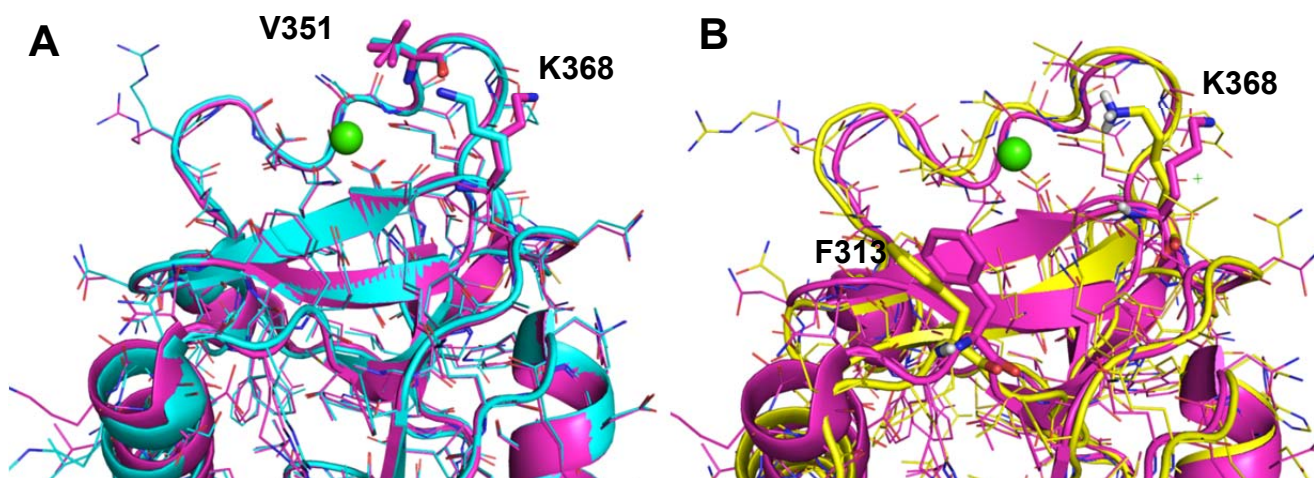


Figure S2. **A)** Superimposition of PDB 2XR5 (magenta) and PDB 2IT5 (cyan) DC-SIGN X-ray crystal structures. **B)** Superimposition of PDB 2XR5 (magenta) and 2XR5-MD (the average structure of PDB 2XR5 from MD simulation, in yellow). Calcium atom is shown as a green sphere.

All the ligands were docked into the three DC-SIGN structures (2XR5, 2IT5 and 2XR5-MD). The ps-diMan ligand **1** (from PDB 2XR5) was used as a reference molecule to validate the docking protocol in the three DC-SIGN structures (predicted binding energy of -3.0 kcal/mol). In most cases, the compounds were predicted to bind similarly to reference ligand **1** (*i.e.* docked pose with mannose oxygens 3 and 4 interacting with the calcium atom). The best results, in terms of predicted binding energy, were obtained in the average structure from the MD simulation (2XR5-MD). We always considered as good predicted poses the ones where the pseudo-dimannoside is placed and interacts with the protein in the same way as compound **1** in PDB 2XR5 (representative example is shown in Figure S3).

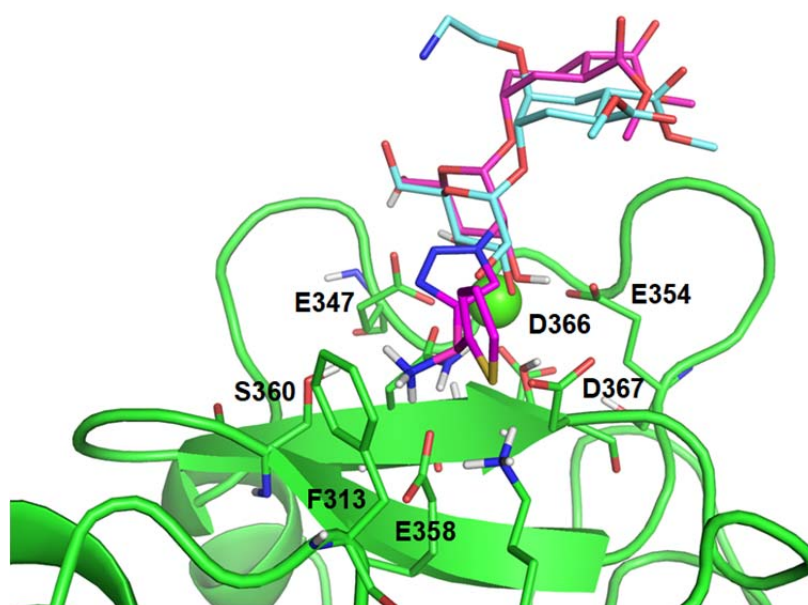


Figure S3. Representative docked pose of compound **5i** (magenta) into DC-SIGN structure from PDB 2XR5. Compound **1** (cyan) from PDB 2XR5 is shown superimposed.

Based on previously reported work,^[1] the *p*-hydroxymethylenebenzylamide moiety was considered for functionalization of ligand **5a**, yielding compound **16**. Docking of this compound afforded a proper docked pose, similar to that reported for compound **1**, and similar to that for compound **16** in PDB 6GHV (see Figure 7C).

MD Simulation of the DC-SIGN/16 complex

DC-SIGN/16 complex from PDB 6GHV was submitted to 100 ns MD simulations. No major changes in both ligand and protein were observed along the simulation time (Figure S4). The mannose residue remained stable and oxygens of carbon 3 and 4 (Man-O3 and Man-O4) interacted during the whole simulation with the calcium ion present in the binding site. The ammonium group of **16** remained interacting with Phe313 and Glu358 side chains during the MD simulation time.

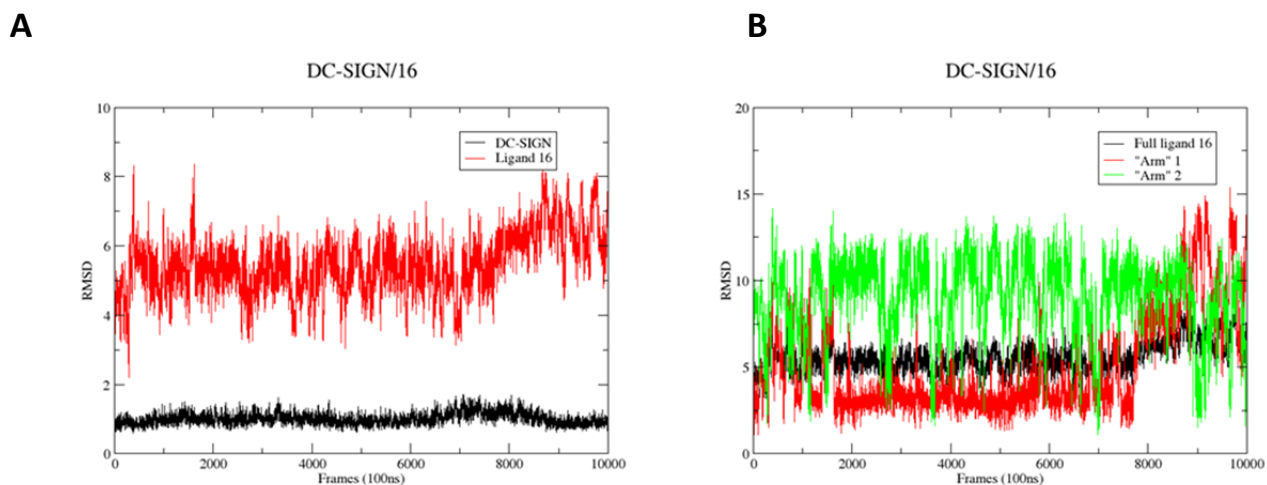


Figure S4. MD simulation of DC-SIGN/16 complex (PDB 6GHV). **A)** RMSD graph during the simulation of the ligand (red lines) and the protein (black lines). **B)** RMSD graph during the simulation of the ligand (black lines) and arms 1 (benzylamide at C5) and 2 (benzylamide at C4) of the ligand (red and green lines, respectively).

SPR Competition assay: inhibition data

DC-SIGN Inhibition properties of compounds.

Table S1. Glycomimetics inhibitory potency towards DC-SIGN. SPR competition assays were performed at pH 8 with 20 μM DC-SIGN ECD, with increasing concentration of ligands. IC_{50} were extracted from inhibition curves as detailed in materials and methods.

Compounds	IC_{50} (μM)
Man	2 404 \pm 5
1	956 \pm 38
2	329 \pm 5
3	254 \pm 5
5a	108 \pm 1
5b	799 \pm 12
5c	240 \pm 1
5d	407 \pm 7
12a	643 \pm 8
12b	672 \pm 3
12c	871 \pm 2
13	180 \pm 5
14	609 \pm 6
15a	339 \pm 7
15b R/S	870 \pm 1
15b S/R	590 \pm 4
16	76 \pm 3

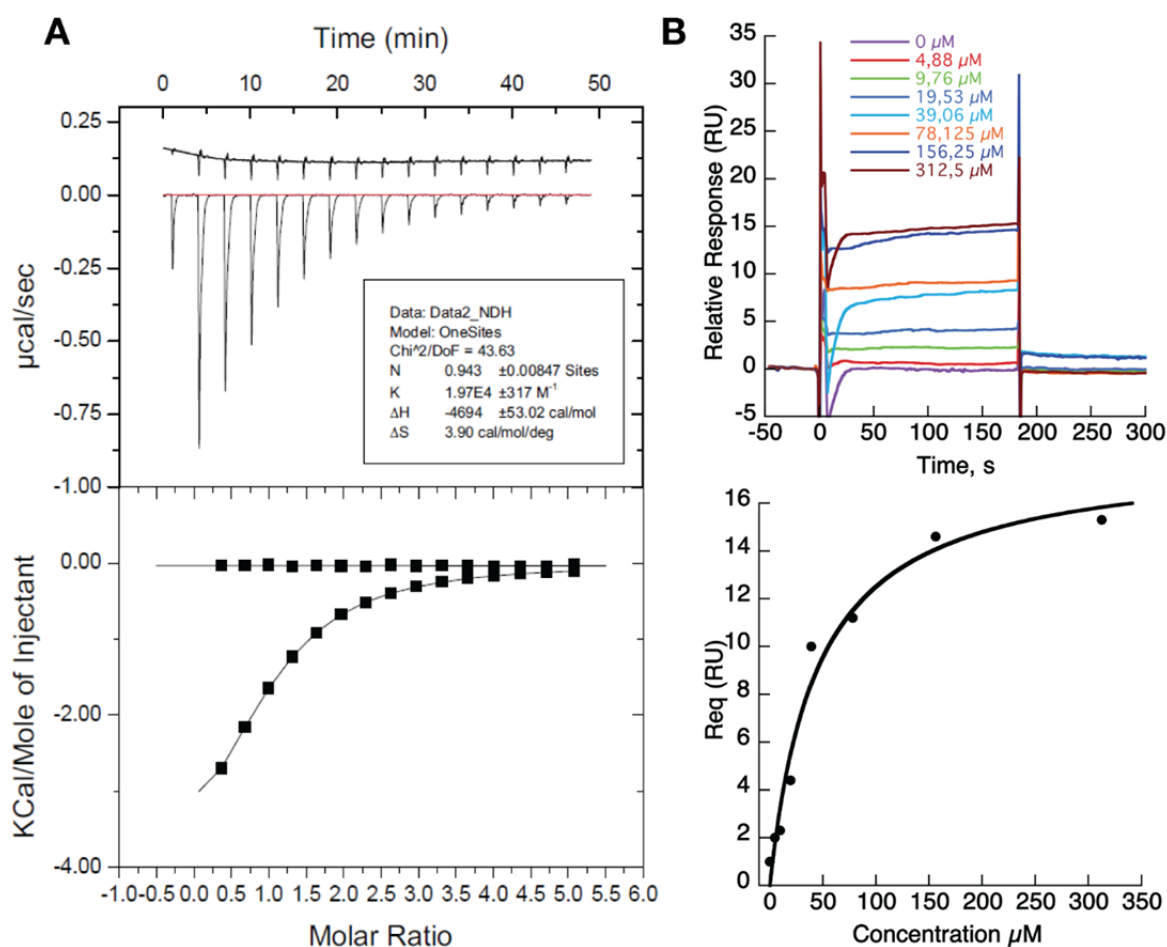
Biophysical characterization of **16** binding to DC-SIGN

Figure S5. Dissociation constants determination by ITC and SPR. Titrations of glycomimetic **16 at 2.5 mM to DC-SIGN ECD solution (100 μM).** A) Upper panel shows the titration thermogram and lower panel, the data integration with fitted curves (1:1 binding model). A control experiments with injections of **16** alone in buffer was performed to remove the contribution of the glycomimetic dilution in the K_d determination. Experiments were repeated twice. B) Titration of glycomimetic **16** onto DC-SIGN ECD functionalized surface. Upper panel shows reference-subtracted sensorgrams of increasing concentrations of **16** (higher concentration from 312 μM down to zero by serial dilution) and lower panel, the steady state binding analysis (1:1 binding model).

Structural analysis

Data processing and structure determination. XDS/XSCALE (version 20180126) programs were used to process data resulting in a $P2_1$ space group, with unit cell parameters (see Table S2) and a data set of 65455 reflections between 40 and 2.1 Å resolution with 98.4% of completeness. Structure was solved by molecular replacement, using 1K9I DC-SIGN CRD structure and MOLREP (version 11.6.2). Model building was made alternating refinement with REFMAC (version 5.8.0218) and manual construction with COOT (version 0.8.9 EL) resulting in a final structure (see Table S2 for the crystal structure parameters).

Table S2. DC-SIGN CRD/16 complex data collection and structure refinement statistics

Data collection statistics	
Wavelength (Å)	0.966
Space group	P12 ₁
Unit cell parameters (Å)	a=105.612, b=57.507, c=107.247 α =90, β =118.666, γ =90
Resolution (Å)	94.1-2.1 (2.2-2.1) ^a
Unique reflections	65455 (8427)
Completeness (%)	98.4 (97.9)
$I/\sigma(I)$	8.47 (2.01)
R_{merge}^b (%)	9.9 (54.5)
Structure refinement statistics	
Resolution (Å)	40-2.1
Refinement factors	
Used reflections/free (%)	62185/3261
R_{cryst}^c	0.1759
R_{free}^c	0.2336
rmsd from ideality	
Bond angles (deg)	1.6610
Bond lengths (Å)	0.0166
Ramachandran plot (%)	
Most favoured regions	97.8
Additional allowed regions	1.4
Disallowed regions	0.8
Average B-factors (Å ²)	33.681

aValues in parentheses are for the highest resolution shell. b $R_{\text{merge}} = \sum_h \sum_m |I_m(h) - \langle I(h) \rangle| / \sum_h \sum_m I_m(h)$. c $R_{\text{work}} = \sum_h ||F_0| - |F_c|| / \sum_h |F_0|$, and $R_{\text{free}} = R_{\text{work}}$ calculated with 5% of randomly isolated F_0 .

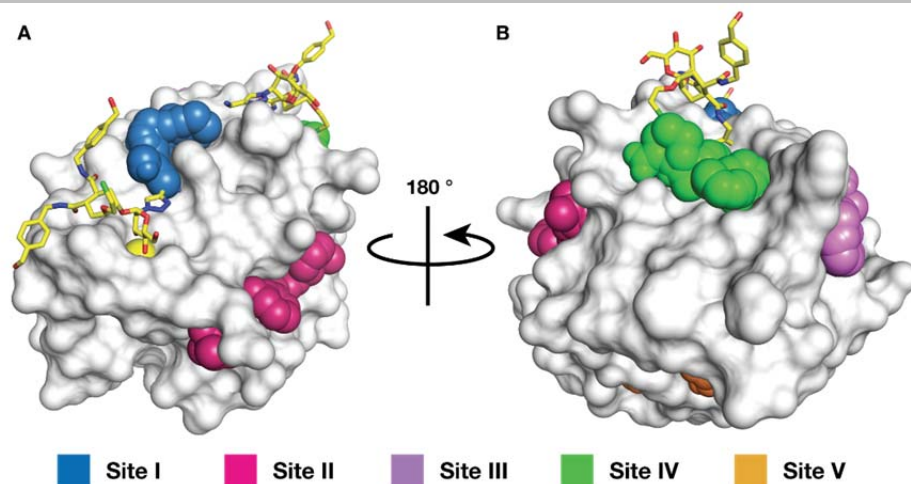


Figure S6: Superposition of DC-SIGN CRD/16 complex and potential secondary druggable binding sites previously identified by Aretz *et al.*^[2] A) In the canonical binding site, the ammonium overlaps with the extremity of the Site I. B) In the non-canonical binding site the p-hydroxymethylenebenzylamide arm dive into the Site IV. In this work we demonstrate that these putative secondary sites can really be exploited by some ligands.

Acknowledgement: we are grateful to C. Rademacher for sharing structural file highlighting the secondary druggable binding sites previously published.

Experimental Procedures

Computational methods

Protein Preparation. X-Ray crystallographic structures of DC-SIGN were obtained from the Protein Data Bank^[3] with PDB codes of 2XR5 and 2IT5. The proteins were prepared using the Protein Preparation Wizard tool included in Maestro.^[4] Water molecules, co-factors of crystallization (three Cl⁻ ions in the case of 2XR5; no co-factors were present in 2IT5) and ligands (pseudo-dimannoside **1** in 2XR5 and α -D-mannose in 2IT5) were removed. Missing atoms and cap termini were added, and hydrogens were added with Epik^[5] at physiological pH. The three structural calcium atoms present in the crystal structure were left, being one of them crucial for the ligand binding. These two completed 3D structures of DC-SIGN were minimized with OPLS3 force field as implemented in Maestro with implicit solvent (water). The final minimized structures were used for docking purposes.

Fragment library preparation. The Maybridge Ro3 core set fragment library^[6] was selected for the virtual screening. The database was prepared using LigPrep.^[7] The 3D structures were optimized using OPLS2005 force field. Original chiralities were retained and possible water or ions present in the structure were removed. Possible tautomers at pH 7 +/- 0.5 were generated with Epik, as well as predicted ionization states for every molecule.

Virtual screening. Virtual screening of the fragment library was performed using GLIDE VS workflow^[8] in the DC-SIGN structure refined from PDB 2XR5. The center of the grid box was placed at the centroid defined among Phe313, Glu358 and Asn365 residues. The inner box size was 8x8x8 Å, and the outer box size was 19x19x19 Å, including the adjacent pocket of the calcium binding site, the so-called "ammonium binding pocket". No excluded volumes were used in the grid preparation. Scaling factor and partial charge cutoff were set as default (0.8 and 0.15, respectively). 20% of the poses were kept in the first stage (High Throughput Virtual Screening, HTVS), 50% in the second step (Standard Precision, SP) and 50% in the last step (Extra Precision, XP).

Ligands building, optimization and parameters calculation. All ligands were built with Maestro and geometries were minimized with OPLS2005 force field. Further optimization was performed with Gaussian^[9] at the Hartree-Fock level of theory RHF/6-31G*. Charges were derived from the optimized geometries, and formatted for AmberTools 4 and AMBER14^[10] with Antechamber by assigning the general AMBER force field (GAFF) atom types.^[11] Parameters for molecular dynamics simulation of the new units were set up with the standard Antechamber procedure.

Docking. Docking of constructed ligands was performed using AutoDock 4 software.^[12] Docking settings were set as default (maximum number of evaluations = 2500000; maximum number of generations = 27000; rate of gene mutation = 0.02; rate of crossover = 0.8). A 3D grid was defined (54x50x56 grid points; grid spacing = 0.375 Å) centered at the centroid among residues Glu347, Glu354 and Asn365, which are at the center of the binding site. The box was defined to ensure that both CRD and ammonium binding site were included. A distance-dependent dielectric constant was used. The original Lennard-Jonnes and

hydrogen-bonding potentials provided by AutoDock were also used. After docking, the 200 solutions were clustered in groups with root-mean-square deviation less than 2.0 Å. The clusters were ranked by the lowest energy representative of each cluster.

Molecular dynamics (MD) simulations. The MD simulations were carried out by using the sander module in AMBER14. GLYCAM06, GAFF, and ff14SB were used as force fields. Counterions (Cl⁻) were added to neutralize the system. Each system was then solvated by using TIP3P waters in a cubic box with at least 10 Å of distance around each protein/ligand complex. The shake algorithm was applied to constrain only bonds involving hydrogen, and an integration step of 1 fs was used. Periodic boundary conditions were applied, as well as the smooth particle mesh Ewald method to represent the electrostatic interactions, with a grid space of 1 Å. Each system was gently annealed from 100 to 300 K over a period of 25 ps. The system was then maintained at temperature of 300 K during 50 ps with solute restraint and progressive energy minimizations, gradually releasing the restraints of the solute followed by a 20 ps heating phase from 100 to 300 K, where restraints were removed. Production simulation for each system lasted 100 ns. Coordinate trajectories were recorded each 2 ps throughout production runs, yielding an ensemble of 5000 structures for each complex, which were finally analyzed.

SYNTHESIS

General experimental

Chemicals were purchased from commercial sources (Sigma-Aldrich or Acros Organics, D-Mannosamine hydrochloride **6** was purchased from Carbosynth) and used without further purification, unless otherwise indicated. When anhydrous conditions were required, the reactions were performed under nitrogen atmosphere. Anhydrous solvents were purchased from Sigma-Aldrich® with water content ≤ 0.005%. TEA, DCM, MeCN and MeOH were dried over calcium hydride, THF was dried over sodium/benzophenone and freshly distilled. Reactions were monitored by analytical thin-layer chromatography (TLC) performed on Silica Gel 60 F254 plates (Merck) or Silica Gel 60 RP-18F254s (Merck) plates with UV detection (254 nm and 365 nm) and/or staining with ammonium molybdate acid solution, potassium permanganate alkaline solution or ninhydrin. Flash column chromatography was performed according to the method of Still and co-workers^[13] using Silica gel 60 (40-63 μm) (Merck).

Automated flash chromatography was performed on an Isolera™ Prime Advanced Automated Flash Purification system (Biotage AB, Uppsala Sweden) employing prepacked Biotage® SNAP KP-C18-HS or Biotage® SNAP KP-Sil cartridges; unless otherwise indicated. For analytical HPLC Waters 515 HPLC pump/996 photodiode array detector was used, while semi-preparative HPLC was carried out on a Thermo Scientific Ultimate 3000 instrument and Waters Atlantis 21 mm x 10 cm column. The final ligands were lyophilized on a Lio5P DGT from 5Pascal, Trezzano Sul Naviglio, Italy. All organic solvents were concentrated using rotary evaporation. The optical rotation values were measured by Perkin-Elmer 241, at 589 nm, in a 1 dm cell.

¹H and ¹³C spectra were acquired on Bruker Avance 400 MHz spectrometer at 298K. Chemical shifts were reported in ppm (δ) and referenced to the residual signal of the solvent used - CDCl₃ (7.26 for ¹H and 77.16 for ¹³C), CD₃OD (3.31 for ¹H and 49.00 for ¹³C), D₂O (4.79 for ¹H). ¹³C spectra in D₂O were referenced directly off the solvent deuterium signal. Splitting patterns are designated as s, singlet; d, doublet; t, triplet; m, multiplet; br s, broad singlet. Coupling constants (*J*) are reported in Hz.

Mass spectra were recorded on a ThermoFischer LCQ apparatus (ESI ionization); high resolution mass spectra (HRMS) were acquired on a Waters SYNAPT G2 Si ESI QToF instrument, (Waters, Manchester, UK) and processed with Waters MassLynx software. The instrument was operated with a capillary voltage of 1.0 – 3.0 kV; sample infusion flow rate: 5 μl/min; source temperature: 100°C; sampling cone: 24.0000V; desolvation temperature: 150°C. Desolvation gas flow was set to 500.0 L/hr; and the nebulizer gas flow to 7.0 Bar. MALDI-ToF mass measurements were performed on an Ultraflextreme III time-of-flight mass spectrometer equipped with a pulsed Nd:YAG laser (λ 355 nm) and controlled by FlexControl 3.3 software (Bruker Daltonics, Bremen, Germany). The acquisitions (total of 2000-3000) were carried out in positive or negative reflector ion extraction of 450 ns and laser frequency of 1000 Hz. Laser fluence was set up to 60-80 % and the *m/z* range was chosen according to the mass of the sample. The accumulated spectra were processed using the Bruker software FlexAnalysis 3.3.

Alkynes used in CuAAC reactions and corresponding triazole derivatives

Alkynes **17a-c**, **18a-b**, **19**, **20** and **21a**, shown in Figure S7, were purchased from Sigma-Aldrich and **21b** was purchased from VWR. Racemic **17d** was synthesized according to Messina *et al.*^[14] and **18c** was synthesized according to Ryu *et al.*^[15]

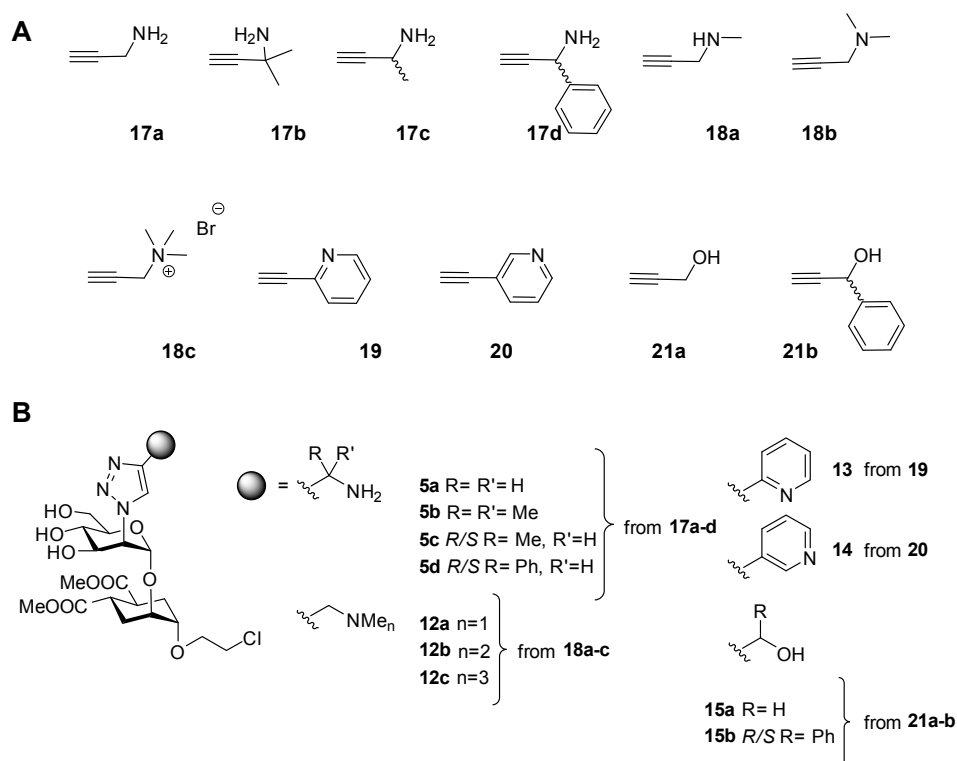
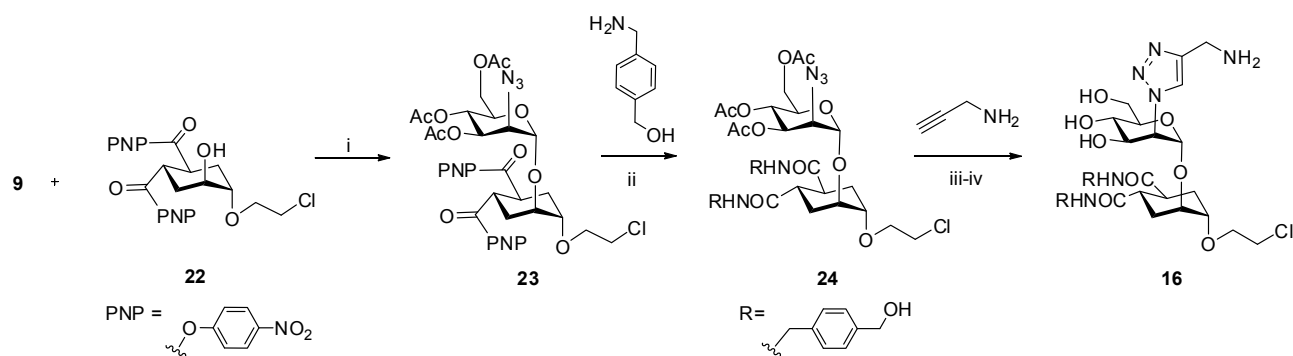
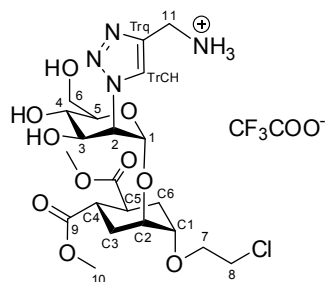


Figure S7. A) Alkynes used in CuAAC reactions with azide **11**. Alkynes **17d** and **18c** were synthesized according to literature (ref 13 and 14), while the rest is commercially available. B) The triazole derivatives synthesized.

Synthesis of **16**

Scheme S1. Synthesis of **16**. i) TMSOTf, mol. sieves, CH₂Cl₂, -30°C, 1h, 82%; ii) THF/DMF, **2d**, 86%; iii) CuSO₄·5H₂O, Na-ascorbate, THF/water; iv) MeONa, MeOH, R.T., 30', 76% over two steps. Acceptor **22** was prepared according to Varga *et al.*^[11b] and Medve *et al.*^[16].

Compound characterization

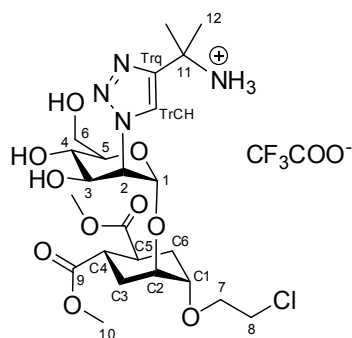
Compound 5a

Synthesized from **11** and **17a** according to the general procedure for CuAAC reactions and Zemplén-deacetylation. Yield: 97% (over two steps). R_f: 0.23 in DCM : MeOH = 8 : 2

¹H-NMR (400 MHz, D₂O): δ = 8.30 (s, 1H, H_{TrCH}), 5.42 (s, 1H, H₁), 5.29 (dd, 1H, H₂, J₁₋₂ = 1.2 Hz, J₂₋₃ = 5.2 Hz), 4.37 (s, 2H, H₁₁), 4.35 (dd, 1H, H₃, J₃₋₄ = 9.5 Hz), 4.14 - 4.12 (m, 1H, C₂), 4.00 - 3.90 (m, 3H, H_{6a,b}, H_{7a}), 3.90 - 3.84 (m, 3H, H_{7b}, H₅, C₁), 3.78 - 3.75 (m, 2H, H_{8a,b}), 3.75 (s, 3H, H₁₀), 3.72 (s, 3H, H₁₀), 3.75 - 3.70 (m, 1H, H₄), 3.06 - 2.96 (m, 2H, C₄, C₅), 2.24 (d, 1H, C_{6eq}, J_{C6eq-C6ax} = 13.8 Hz), 2.15 (d, 1H, C_{3eq}, J_{C3eq-C3ax} = 14.6 Hz), 2.00 - 1.84 (m, 2H, C_{6ax}, C_{3ax}).

¹³C-NMR (100 MHz, D₂O): δ = 177.5 (C₉), 177.2 (C₉), 139.7 (C_{Trq}), 125.7 (C_{TrCH}), 95.9 (C₁), 74.2 (C_{C1} or C₅), 73.7 (C₅ or C_{C1}), 71.2 (C_{C2}), 69.0 (C₇), 68.5 (C₃), 66.3 (C₄), 63.9 (C₂), 60.4 (C₆), 52.7 (C₁₀), 43.6 (C₈), 39.0 (C_{C4}, C_{C5}), 34.0 (C₁₁), 27.1 (C_{C6}), 26.4 (C_{C3}).

MS (ESI): *m/z* calculated for [C₂₁H₃₃ClN₄O₁₀Na]⁺: 559.18 [M + Na]⁺, found: 559.43; calculated for [C₂₁H₃₄ClN₄O₁₀]⁺: 537.20 [M + Na]⁺, found: 537.42

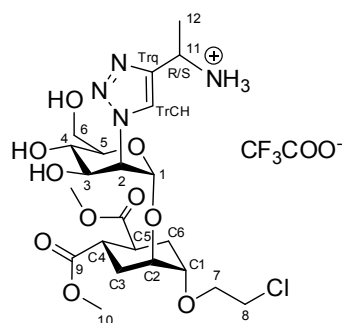
Compound 5b

Synthesized from **11** and **17b** according to the general procedure for CuAAC reactions and Zemplén-deacetylation. Yield: 62% (over two steps). R_f: 0.11 in DCM : MeOH = 1 : 1 + 0.01% TFA

¹H NMR (400 MHz, CD₃OD): δ = 8.29 (s, 1H, H_{TrCH}), 5.26 (d, 1H, H₁, J₁₋₂ = 1.5 Hz), 5.16 (dd, 1H, H₂, J₂₋₁ = 1.5 Hz, H₂₋₃ = 5.0 Hz), 4.18 (dd, 1H, H₃, J₃₋₄ = 8.9 Hz, J₃₋₂ = 5.0 Hz), 4.06 - 4.03 (m, 1H, C₂), 3.88 - 3.70 (m, 9H, H₄, H₅, H_{6a,b}, H_{7a,b}, C₁, H_{8a,b}), 3.66 (s, 3H, H₁₀), 3.63 (s, 3H, H₁₀), 2.99 - 2.81 (m, 2H, C₄, C₅), 2.17 - 2.01 (m, 2H, C_{3ax}, C_{6ax}), 1.88 - 1.77 (m, 2H, C_{3eq}, C_{6eq}), 1.74 (s, 6H, H₁₂)

¹³C NMR (100 MHz, CD₃OD): δ = 177.0 (C₉); 176.7 (C₉); 140.7 (C_{Trq}); 123.5 (C_{TrCH}); 98.0 (C₁); 76.0 (C_{C1} or C₅); 75.9 (C₅ or C_{C1}); 73.0 (C_{C2}); 70.8 (C₇); 70.4 (C₃); 67.9 (C₄); 65.8 (C₂); 61.9 (C₆); 52.7 (C₁₁); 52.5 (C₁₀); 44.4 (C₈); 40.5 (C_{C4} or C_{C5}); 40.3 (C_{C5} or C_{C4}); 29.2 (C_{C6} or C_{C3}); 28.2 (C_{C3} or C_{C6}); 27.2, 27.0 (C₁₂)

MS (HRMS): *m/z* calculated for [C₂₃H₃₇ClN₄O₁₀]⁺: 587.2090 [M + Na]⁺, found: 587.2096

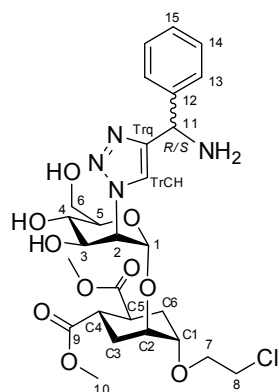
Compound 5c

Synthesized from **11** and **17c** according to the general procedure for CuAAC reactions and Zemplén-deacetylation. Yield: 31% (over two steps). *R_f*: 0.19 in water : MeOH = 1 : 1 + 0.01% TFA (both diastereomers)

¹H NMR (400 MHz, CD₃OD): δ = 8.31 (s, 1H, H_{TrCH}), 5.31 (d, 1H, H₁, *J*₁₋₂ = 1.5 Hz), 5.16 (dd, 1H, H₂, *J*₂₋₁ = 1.5 Hz, H₂₋₃ = 5.0 Hz), 4.70 (dd, 1H, H₁₁, *J*₁₁₋₁₂ = 6.9 Hz, *J* = 13.6 Hz), 4.23 (dd, 1H, H₃, *J*₃₋₄ = 8.6 Hz, *J*₃₋₂ = 5.0 Hz), 4.12 - 4.08 (m, 1H, C₂), 3.93 - 3.73 (m, 9H, H₄, H₅, H_{6a,b}, H_{7a,b}, C₁, H_{8a,b}), 3.71 (s, 3H, H₁₀), 3.68 (s, 3H, H₁₀), 3.04 - 2.84 (m, 2H, C₄, C₅), 2.21 - 2.05 (m, 2H, C_{3ax,6ax}), 1.93 - 1.82 (m, 2H, C_{3eq,6eq}), 1.74 (s, 6H, H₁₂), 1.72 (s, 6H, H₁₂)

¹³C NMR (100 MHz, CD₃OD): δ = 176.8 (C₉); 176.5 (C₉); 142.0 (C_{Trq}); 124.4 (C_{TrCH}); 97.8 (C₁); 75.8 (C_{C1} or C₅); 75.7 (C₅ or C_{C1}); 72.8 (C_{C2}); 70.6 (C₇); 70.3 (C₃); 67.9 (C₄); 65.5 (C₂); 61.9 (C₆); 52.3 (C₁₀); 44.5 (C₈); 44.1 (C₁₁); 40.3 (C_{C4} or C_{C5}); 40.1 (C_{C5} or C_{C4}); 29.0 (C_{C6} or C_{C3}); 28.0 (C_{C3} or C_{C6}); 19.0, 18.9 (C₁₂)

MS (HRMS): *m/z* calculated for [C₂₂H₃₆ClN₄O₁₀]⁺: 585.1958 [M + H]⁺, found: 585.1961

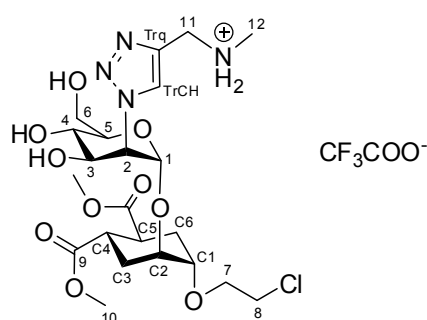
Compound 5d

Synthesized from **11** and **21b** according to the general procedure for CuAAC reactions and Zemplén-deacetylation. Yield: 86% (over two steps). *R_f*: 0.33 in water : MeOH = 1 : 1 (both diastereomers)

¹H NMR (400 MHz, CD₃OD): δ = 8.09 (s, 1H, H_{TrCH}), 8.07 (s, 1H, H_{TrCH}), 7.48 - 7.43 (m, 2H, H₁₃), 7.41 - 7.34 (m, 2H, H₁₄), 7.33 - 7.27 (m, 1H, H₁₅), 5.33 - 5.30 (m, 2H, H₁₁, H₁), 5.11 (dd, 1H, H₂, *J*₂₋₁ = 1.6 Hz, H₂₋₃ = 4.9 Hz), 4.19 (dd, 1H, H₃, *J*₃₋₄ = 8.7 Hz, *J*₃₋₂ = 4.9 Hz), 4.11 - 4.07 (m, 1H, C₂), 3.94 - 3.74 (m, 9H, H₄, H₅, H_{6a,b}, H_{7a,b}, C₁, H_{8a,b}), 3.71 (s, 3H, H₁₀), 3.68 (s, 3H, H₁₀), 3.03 - 2.87 (m, 2H, C₄, C₅), 2.21 - 2.06 (m, 2H, C_{3ax}, C_{6ax}), 1.93 - 1.81 (m, 2H, C_{3eq}, C_{6eq})

¹³C NMR (100 MHz, CD₃OD): δ = 177.5 (C₉); 177.2 (C₉); 138.0 (C_{Trq}); 130.1 (C₁₃); 129.6 (C₁₅); 128.6 (C₁₄); 126.8 (C_{TrCH}); 99.3 (C₁); 77.0 (C_{C1} or C₅); 76.7 (C₅ or C_{C1}); 74.1 (C_{C2}); 71.7 (C₇); 71.4 (C₃); 70.8 (C₁₁); 69.0 (C₄); 66.6 (C₂); 63.2 (C₆); 53.4 (C₁₀); 45.3 (C₈); 41.4, 41.2 (C_{C4}, C_{C5}); 30.1 (C_{C6}); 29.2 (C_{C3})

MS (HRMS): *m/z* calculated for [C₂₇H₃₈ClN₄O₁₀]⁺: 613.2271 [M + H]⁺, found: 613.2274

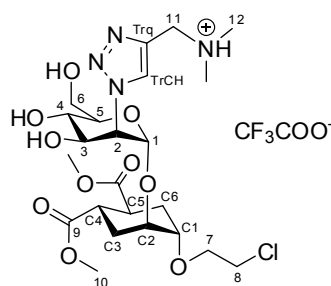
Compound 12a

Synthesized from **11** and **18a** according to the general procedure for CuAAC reactions and Zemplén-deacetylation. Yield: 75% (over two steps). R_f: 0.06 in water : MeOH = 1 : 1 + 0.01% TFA

¹H NMR (400 MHz, D₂O): δ = 8.36 (s, 1H, H_{TrCH}), 5.42 (s, 1H, H₁), 5.30 (d, 1H, H₂, J₁₋₂ = 4.9 Hz), 4.42 (s, 2H, H₁₁), 4.36 (dd, 1H, H₃, J₃₋₄ = 9.5 Hz, J = 4.9 Hz), 4.17 - 4.11 (m, 1H, C₂), 4.00 - 3.83 (m, 6H, H₅, H_{6a,b}, H_{7a,b}, C₁), 3.78 - 3.75 (m, 2H, H_{8a,b}), 3.75 (s, 3H, H₁₀), 3.72 (s, 3H, H₁₀), 3.75 - 3.72 (m, 1H, H₄), 3.06 - 2.96 (m, 2H, C₄, C₅), 2.79 (s, 3H, H₁₂), 2.28 - 2.10 (m, 2H, C_{3ax}, C_{6ax}), 2.03 - 1.84 (m, 2H, C_{3ax}, C_{6ax})

¹³C NMR (100 MHz, D₂O): δ = 177.5 (C₉); 177.2 (C₉); 138.0 (C_{Trq}); 126.8 (C_{TrCH}); 96.0 (C₁); 74.3 (C_{C1} or C₅); 73.8 (C₅ or C_{C1}); 71.4 (C_{C2}); 69.1 (C₇); 68.6 (C₃); 66.4 (C₄); 64.0 (C₂); 60.5 (C₆); 52.8 (C₁₀); 43.7 (C₈); 42.7 (C₁₁); 39.1 (C_{C4}, C_{C5}); 34.0 (C₁₂); 27.2 (C_{C6}); 26.4 (C_{C3})

MS (ESI): *m/z* calculated for [C₂₂H₃₆ClN₄O₁₀]⁺: 551.21 [M + H]⁺, found: 551.07

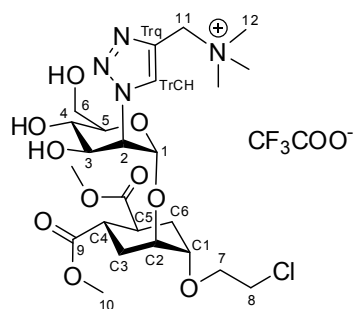
Compound 12b

Synthesized from **11** and **18b** according to the general procedure for CuAAC reactions and Zemplén-deacetylation. Yield: 84% (over two steps). R_f: 0.1 in water : MeOH = 1 : 1 + 0.01% TFA

¹H NMR (400 MHz, D₂O): δ = 8.38 (s, 1H, H_{TrCH}), 5.36 (s, 1H, H₁), 5.25 (d, 1H, H₂, J₁₋₂ = 5.1 Hz, J₂₋₃ = 1.2 Hz), 4.46 (s, 2H, H₁₁), 4.33 (dd, 1H, H₃, J₃₋₄ = 9.5 Hz, J = 5.0 Hz), 4.10 - 4.05 (m, 1H, C₂), 3.92 - 3.77 (m, 6H, H₅, H_{6a,b}, H_{7a,b}, C₁), 3.71 - 3.69 (m, 2H, H_{8a,b}), 3.68 (s, 3H, H₁₀), 3.65 (s, 3H, H₁₀), 3.68 - 3.65 (m, 1H, H₄), 3.00 - 2.90 (m, 2H, C₄, C₅), 2.79 (app d, 6H, H₁₂), 2.23 - 2.03 (m, 2H, C_{3ax}, C_{6ax}), 1.97 - 1.76 (m, 2H, C_{3ax}, C_{6ax})

¹³C NMR (100 MHz, D₂O): δ = 177.5 (C₉); 177.2 (C₉); 136.4 (C_{Trq}); 127.9 (C_{TrCH}); 95.9 (C₁); 74.2 (C_{C1} or C₅); 73.7 (C₅ or C_{C1}); 71.2 (C_{C2}); 69.0 (C₇); 68.4 (C₃); 66.3 (C₄); 64.0 (C₂); 60.3 (C₆); 52.7 (C₁₀); 51.1 (C₈); 43.6 (C₁₁); 42.1 (C_{C4}, C_{C5}); 39.0 (C₁₂); 27.2 (C_{C6}); 26.4 (C_{C3})

MS (ESI): *m/z* calculated for [C₂₃H₃₈ClN₄O₁₀]⁺: 565.23 [M + H]⁺, found: 565.02

Compound 12c

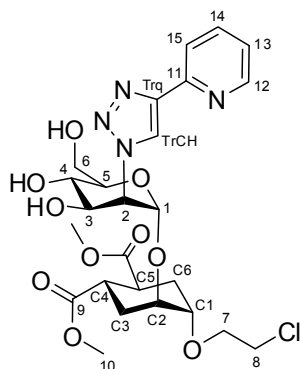
Synthesized from **11** and **18c** according to the general procedure for CuAAC reactions and Zemplén-deacetylation. Yield: 53% (over two steps). R_f: 0.26 in water : MeOH = 1 : 1 + 0.01% TFA

¹H NMR (400 MHz, CD₃OD): δ = 8.08 (s, 1H, H_{TrCH}), 5.27 (s, 1H, H₁), 5.26 (d, 1H, H₂, J₁₋₂ = 5.1 Hz, J₂₋₃ = 1.0 Hz), 4.53 (s, 2H, H₁₁), 4.21 (dd, 1H, H₃, J₃₋₄ = 9.6 Hz, J = 5.3 Hz), 3.99 - 3.95 (m, 1H, C₂), 3.81 - 3.66 (m, 6H, H₅, H_{6a,b}, H_{7a,b}, C₁), 3.61 - 3.59 (m, 2H, H_{8a,b}), 3.58 (s, 3H, H₁₀), 3.55 (s, 3H, H₁₀), 3.58 - 3.55 (m, 1H, H₄), 3.01 (s, 9H, H₁₂), 3.00 - 2.90 (m, 2H, C₄, C₅), 2.01 - 1.94 (m, 2H, C_{3ax}, C_{6ax}), 1.85 - 1.67 (m, 2H, C_{3ax}, C_{6ax})

^{13}C NMR (100 MHz, CD_3OD): δ = 177.5 (C_9); 177.2 (C_9); 135.5 (C_{Trq}); 129.3 (C_{TrCH}); 96.0 (C_1); 74.4 (C_{C_1} or C_5); 73.9 (C_5 or C_{C_1}); 71.4 (C_{C_2}); 69.2 (C_7); 68.6 (C_3); 66.4 (C_4); 64.3 (C_2); 60.4 (C_6); 59.9 (C_{11}); 52.8 (C_8); 52.7 (C_{12}); 43.8 (C_{10}); 39.3 (C_{C_4} , C_{C_5}); 27.2 (C_{C_6}); 26.4 (C_{C_3})

MS (ESI): m/z calculated for $[\text{C}_{24}\text{H}_{40}\text{ClN}_4\text{O}_{10}]^+$: 579.24 $[\text{M} + \text{H}]^+$, found: 579.06

Compound 13



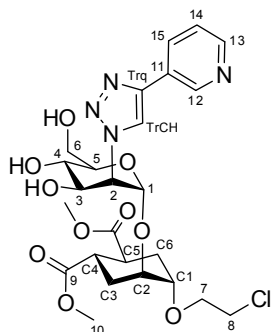
Synthesized from **11** and **19** according to the general procedure for CuAAC reactions and Zemplén-deacetylation. Yield: 77% (over two steps). R_f : 0.11 in water : MeOH = 1 : 1

^1H NMR (400 MHz, D_2O): δ = 8.61 (s, 1H, H_{TrCH}), 8.51 (br s, 1H, H_{12}), 8.01 – 7.92 (m, 2H, H_{13} , H_{15}), 7.47 – 7.39 (m, 1H, H_{14}), 5.46 (d, 1H, H_1 , J_{1-2} = 1.7 Hz), 5.28 (dd, 1H, H_2 , J_{1-2} = 1.7 Hz, J_{2-3} = 5.1 Hz), 4.34 (dd, 1H, H_3 , J_{3-4} = 9.1 Hz, J = 5.1 Hz), 4.15 - 4.11 (m, 1H, C_2), 3.98 - 3.79 (m, 6H, H_5 , $\text{H}_{6\text{a,b}}$, $\text{H}_{7\text{a,b}}$, C_1), 3.79 - 3.70 (m, 3H, $\text{H}_{8\text{a,b}}$, H_4), 3.70 (s, 3H, H_{10}), 3.62 (s, 3H, H_{10}), 3.01 - 2.86 (m, 2H, C_4 , C_5), 2.24 – 2.08 (m, 2H, $\text{C}_{3\text{ax}}$, $\text{C}_{6\text{ax}}$), 1.98 – 1.78 (m, 2H, $\text{C}_{3\text{eq}}$, $\text{C}_{6\text{eq}}$)

^{13}C NMR (100 MHz, D_2O): δ = 177.4 (C_9); 177.2 (C_{11}); 149.0 (C_{12}); 138.7 (C_{Trq}); 138.7 (C_{15}); 124.0 (C_{13}); 123.6 (C_{TrCH}); 121.0 (C_{14}); 95.8 (C_1); 74.2 (C_{C_1} or C_5); 74.1 (C_5 or C_{C_1}); 71.2 (C_{C_2}); 69.0 (C_7); 68.8 (C_3); 66.7 (C_4); 63.9 (C_2); 60.6 (C_6); 52.6 (C_{10}); 43.6 (C_8); 39.0, 38.9 (C_{C_4} , C_{C_5}); 27.1 (C_{C_6} or C_{C_3}); 26.4 (C_{C_3} or C_{C_6})

MS (HRMS): m/z calculated for $[\text{C}_{25}\text{H}_{34}\text{ClN}_4\text{O}_{10}]^+$: 585.1958 $[\text{M} + \text{H}]^+$, found: 585.1961

Compound 14

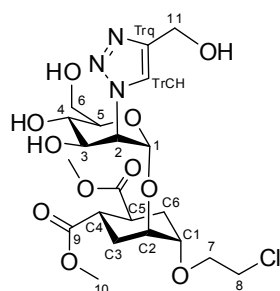


Synthesized from **11** and **20** according to the general procedure for CuAAC reactions and Zemplén-deacetylation. Yield: 45% (over two steps). R_f : 0.19 in water : MeOH = 1 : 1

^1H NMR (400 MHz, CD_3OD): δ = 9.03 (br s, 1H, H_{12}), 8.70 (s, 1H, H_{TrCH}), 8.52 (d, 1H, H_{13} , J_{13-14} = 4.3 Hz), 8.30 (dt, 1H, H_{15} , J = 1.8 Hz, J = 8.0 Hz), 7.53 (dd, 1H, H_{14} , J = 4.8 Hz, J = 8.0 Hz), 5.37 (d, 1H, H_1 , J_{1-2} = 1.7 Hz), 5.18 (dd, 1H, H_2 , J_{1-2} = 1.8 Hz, J_{2-3} = 5.0 Hz), 4.22 (dd, 1H, H_3 , J_{3-4} = 8.5 Hz, J = 5.0 Hz), 4.11 - 4.07 (m, 1H, C_2), 3.96 - 3.73 (m, 6H, H_5 , $\text{H}_{6\text{a,b}}$, $\text{H}_{7\text{a,b}}$, C_1), 3.69 - 3.68 (m, 1H, H_4), 3.68 (s, 3H, H_{10}), 3.68 - 3.64 (m, 2H, $\text{H}_{8\text{a,b}}$), 3.63 (s, 3H, H_{10}), 3.00 - 2.84 (m, 2H, C_4 , C_5), 2.19 – 2.06 (m, 2H, $\text{C}_{3\text{ax}}$, $\text{C}_{6\text{ax}}$), 1.91 – 1.79 (m, 2H, $\text{C}_{3\text{eq}}$, $\text{C}_{6\text{eq}}$)

^{13}C NMR (100 MHz, CD_3OD): δ = 177.4 (C_9); 177.2 (C_9); 148.2 (C_{12}); 138.7 (C_{Trq}); 136.1 (C_{13}); 123.6 (C_{TrCH}); 122.0 (C_{15}); 121.2 (C_{14}); 112.2 (C_{11}); 99.1 (C_1); 77.0 (C_{C_1} or C_5); 76.9 (C_5 or C_{C_1}); 71.7 (C_{C_2}); 71.5 (C_7); 68.9 (C_3); 66.8 (C_4); 62.9 (C_2); 58.6 (C_6); 53.4 (C_{10}); 45.3 (C_8); 41.3, 41.2 (C_{C_4} , C_{C_5}); 30.1 (C_{C_6} or C_{C_3}); 29.1 (C_{C_3} or C_{C_6})

MS (ESI): m/z calculated for $[\text{C}_{25}\text{H}_{34}\text{ClN}_4\text{O}_{10}]^+$: 585.20 $[\text{M} + \text{H}]^+$, found: 587.99

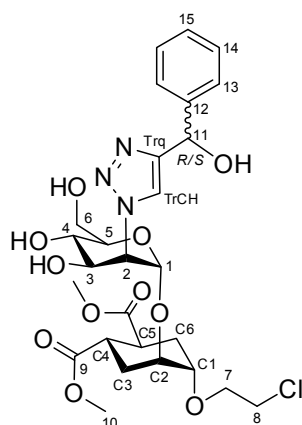
Compound 15a

Synthesized from **11** and **21a** according to the general procedure for CuAAC reactions and Zemplén-deacetylation. Yield: 50% (over two steps). R_f : 0.41 in DCM : MeOH = 9 : 1

$^1\text{H-NMR}$ (400 MHz, D_2O): δ = 8.17 (s, 1H, H_{TrCH}), 5.40 (s, 1H, H_1), 5.23 (dd, 1H, H_2 , J_{1-2} = 1.0 Hz, J_{2-3} = 5.1 Hz), 4.74 (s, 2H, H_{11}), 4.31 (dd, 1H, H_3 , J_{3-4} = 9.6 Hz), 4.12 (m, 1H, C_2), 3.97 - 3.86 (m, 3H, $\text{H}_{6a,b}$, H_{7a}), 3.86 - 3.82 (m, 3H, H_{7b} , H_5 , C_1), 3.77 - 3.73 (m, 2H, $\text{H}_{8a,b}$), 3.73 (s, 3H, H_{10}), 3.70 (s, 3H, H_{10}), 3.73 - 3.69 (m, 1H, H_4), 3.03 - 2.95 (m, 2H, C_4 , C_5), 2.22 (d, 1H, $\text{C}_{6\text{eq}}$, $J_{\text{C}_{6\text{eq}}-\text{C}_{6\text{ax}}} = 14.1$ Hz), 2.14 (d, 1H, $\text{C}_{3\text{eq}}$, $J_{\text{C}_{3\text{eq}}-\text{C}_{3\text{ax}}} = 14.6$ Hz), 1.95 (m, 1H, $\text{C}_{6\text{ax}}$), 1.86 (m, 1H, $\text{C}_{3\text{ax}}$).

$^{13}\text{C-NMR}$ (100 MHz, D_2O): δ = 177.5 (C_9), 177.2 (C_9), 146.7 (C_{Trq}), 124.4 (C_{TrCH}), 96.0 (C_1), 74.2 (C_{C_1} or C_5), 73.7 (C_5 or C_{C_1}), 71.2 (C_{C_2}), 69.0 (C_7), 68.6 (C_3), 66.3 (C_4), 63.7 (C_2), 60.5 (C_6), 54.6 (C_{11}), 52.6 (C_{10}), 43.5 (C_8), 38.9 (C_{C_4} , C_{C_5}), 27.1 (C_{C_6}), 26.4 (C_{C_3}).

MS (ESI): m/z calculated for $[\text{C}_{21}\text{H}_{32}\text{ClN}_3\text{O}_{11}\text{Na}]^+$: 560.16 [$\text{M} + \text{Na}$] $^+$, found: 560.65; calculated for $[\text{C}_{21}\text{H}_{33}\text{ClN}_3\text{O}_{11}]^+$: 538.18 [$\text{M} + \text{Na}$] $^+$, found: 538.67

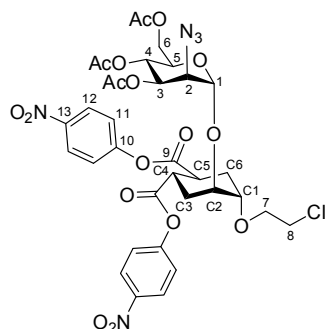
Compounds 15b *R/S* and *S/R*

Synthesized from **11** and **21b** according to the general procedure for CuAAC reactions and Zemplén-deacetylation. Yield: 65% (over two steps). R_f (***R/S***): 0.26; R_f (***S/R***): 0.22 in DCM : MeOH = 94 : 6

$^1\text{H NMR}$ (400 MHz, CD_3OD): δ = 8.08 (s, 1H, H_{TrCH} , (***R/S***)), 8.06 (s, 1H, H_{TrCH} , (***S/R***)), 7.51 - 7.46 (m, 2H, H_{13}), 7.41 - 7.35 (m, 2H, H_{14}), 7.33 - 7.27 (m, 1H, H_{15}), 5.87 (s, 1H, H_{11} , (***R/S***)), 5.86 (s, 1H, H_{11} , (***S/R***)), 5.31 (d, 1H, H_1 , J_{1-2} = 1.4 Hz, (***R/S***)), 5.29 (d, 1H, H_1 , J_{1-2} = 1.4 Hz (***S/R***)), 5.10 (dd, 1H, H_2 , J_{1-2} = 1.4 Hz, J_{2-3} = 5.0 Hz), 4.19 (dd, 1H, H_3 , J_{3-4} = 9.0 Hz, J = 5.0 Hz), 4.11 - 4.06 (m, 1H, C_2), 3.93 - 3.72 (m, 9H, H_4 , H_5 , $\text{H}_{6a,b}$, $\text{H}_{7a,b}$, C_1 , $\text{H}_{8a,b}$), 3.71 (s, 3H, H_{10}), 3.68 (s, 3H, H_{10}), 3.03 - 2.87 (m, 2H, C_4 , C_5), 2.21 - 2.06 (m, 2H, $\text{C}_{3\text{ax}}$, $\text{C}_{6\text{ax}}$), 1.93 - 1.81 (m, 2H, $\text{C}_{3\text{eq}}$, $\text{C}_{6\text{eq}}$)

$^{13}\text{C NMR}$ (100 MHz, CD_3OD): δ = 177.5 (C_9); 177.2 (C_9); 138.0 (C_{Trq}); 130.4 (C_{13}); 129.7 (C_{15}); 128.7 (C_{14}); 126.8 (C_{TrCH}); 99.3 (C_1); 77.0 (C_{C_1} or C_5); 76.7 (C_5 or C_{C_1}); 74.1 (C_{C_2}); 71.7 (C_7); 71.4 (C_3); 71.2 (C_{11}); 69.0 (C_4); 66.6 (C_2); 63.2 (C_6); 53.4 (C_{10}); 45.3 (C_8); 41.4, 41.2 (C_{C_4} , C_{C_5}); 30.1 (C_{C_6}); 29.2 (C_{C_3})

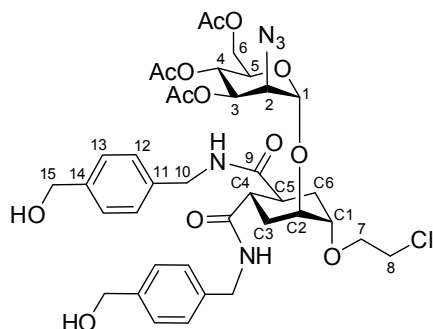
MS (ESI): m/z calculated for $[\text{C}_{27}\text{H}_{36}\text{ClN}_3\text{NaO}_{11}]^+$: 636.19 [$\text{M} + \text{Na}$] $^+$, found: 636.19

Synthesis of **16****Compound 23**

A mixture of the acceptor **22** (79 mg, 0.1549 mmol, 1 mol equiv) and the donor **9** (74 mg, 0.1549 mmol, 1 mol equiv) was co-evaporated with toluene three times. Powdered and activated 4Å molecular sieves (acid washed) were added. The mixture was kept under vacuum for a few hours and then dissolved in dry DCM (2 mL). After cooling to -30°C, TMSOTf (5.6 µL, 0.0310 mmol, 0.2 mol equiv) was added to the stirred mixture. The solution was stirred at -30°C for 1 hour and upon completion, the reaction was quenched with TEA. The mixture was warmed to room temperature and filtered over a celite pad. The filtrate was evaporated at reduced pressure and the crude product was purified by flash chromatography (toluene with a gradient of EtOAc from 0 to 10%) to yield the pure product **23** as a white foam. Yield: 82%.

R_f: 0.25 in hexane : EtOAc = 6 : 4

¹H NMR (400 MHz, CDCl₃): δ = 8.30 – 8.25 (m, 4H, H₁₂), 7.30 – 7.24 (m, 4H, H₁₁), 5.42 – 5.27 (m, 2H, H₃, H₄), 5.07 (d, 1H, H₁, J₁₋₂ = 1.6 Hz), 4.25 (dd, 1H, H_{6a}, J_{6b-5} = 5.6 Hz, J_{6a-6b} = 12.3 Hz), 4.16 – 4.09 (m, 4H, H₂, H_{6b}, C₁, C₂), 3.98 – 3.90 (m, 1H, H_{7a,b}), 3.83 – 3.75 (m, 1H, H₅), 3.68 (t, 2H, H_{8a,b}, J = 5.5 Hz), 2.45 – 3.67 (m, 1H, C₄ or C₅), 3.27 – 3.18 (m, 1H, C₅ or C₄), 2.48 – 2.32 (m, 4H, C_{3eq}, C_{6eq}), 2.20 – 2.13 (m, 4H, C_{3ax}, C_{6ax}), 2.12 (s, 3H, OAc), 2.11 (s, 3H, OAc), 2.08 (s, 3H, OAc).

Compound 24

The PNP-ester **23** (104 mg, 0.1263 mmol, 1 mol equiv) was dissolved in dry DMF (150 µL), diluted with dry THF (1 mL) and (4-hydroxymethylene)benzylamine (52 mg, 0.38 mmol, 3 mol equiv) was added. The reaction was stirred at RT overnight, then, upon completion, the solvent was evaporated. The crude product was purified by flash chromatography (DCM with a gradient of MeOH from 0 to 10%) to yield the pure product **24** as a white foam.

Yield: 86%

R_f: 0.13 in DCM : MeOH = 97 : 3

¹H NMR (400 MHz, CDCl₃): δ = 7.29 – 7.15 (m, 8H, H₁₂, H₁₃), 6.34 (m, 1H, NH), 6.09 (m, 1H, NH), 5.36 – 5.27 (m, 2H, H₃, H₄), 4.95 (d, 1H; H₁, J₁₋₂ = 1.6 Hz), 4.68 – 4.60 (m, 4H, H₁₅), 4.35 – 4.30 (m, 4H, H₁₀), 4.21 (dd, 1H, H_{6a}, J_{6b-5} = 5.1 Hz, J_{6a-6b} = 10.2 Hz), 4.11 – 4.03 (m, 2H, H₂, C₂), 3.98 – 3.92 (m, 2H; H_{6b}, C₁), 3.77 – 3.72 (m, 1H; H_{7a,b}), 3.69 – 3.65 (m, 1H, H₅), 3.60 (t, 2H, H_{8a,b}, J = 5.6 Hz), 2.89 – 2.70 (m, 2H, C₄, C₅), 2.20 – 1.81 (m, 4H, C₃, C₆)

Compound **24** was deacetylated under the general conditions for Zemplén-deacetylation to yield **16** (as described in the main text).

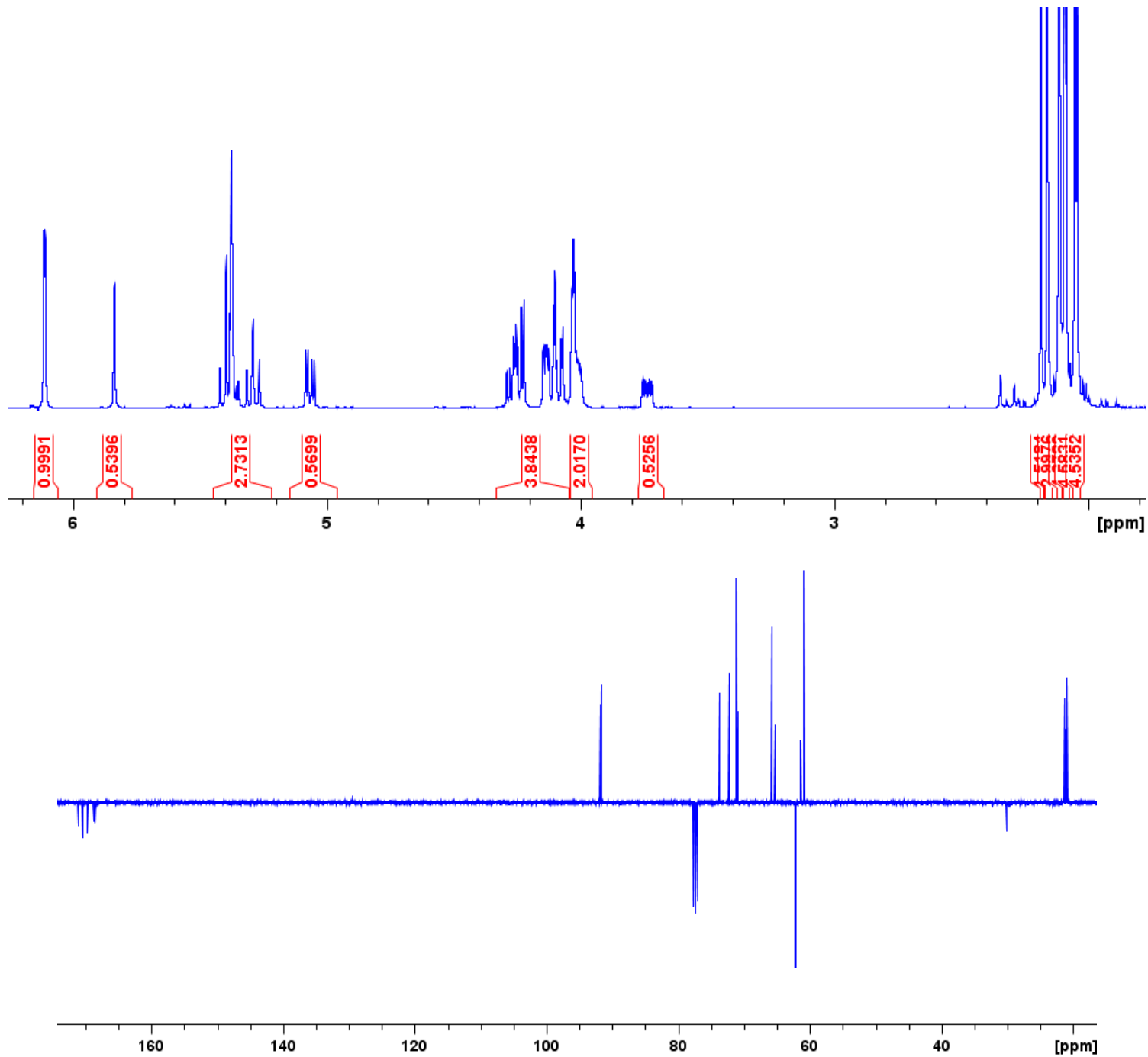
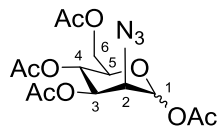
Author Contributions

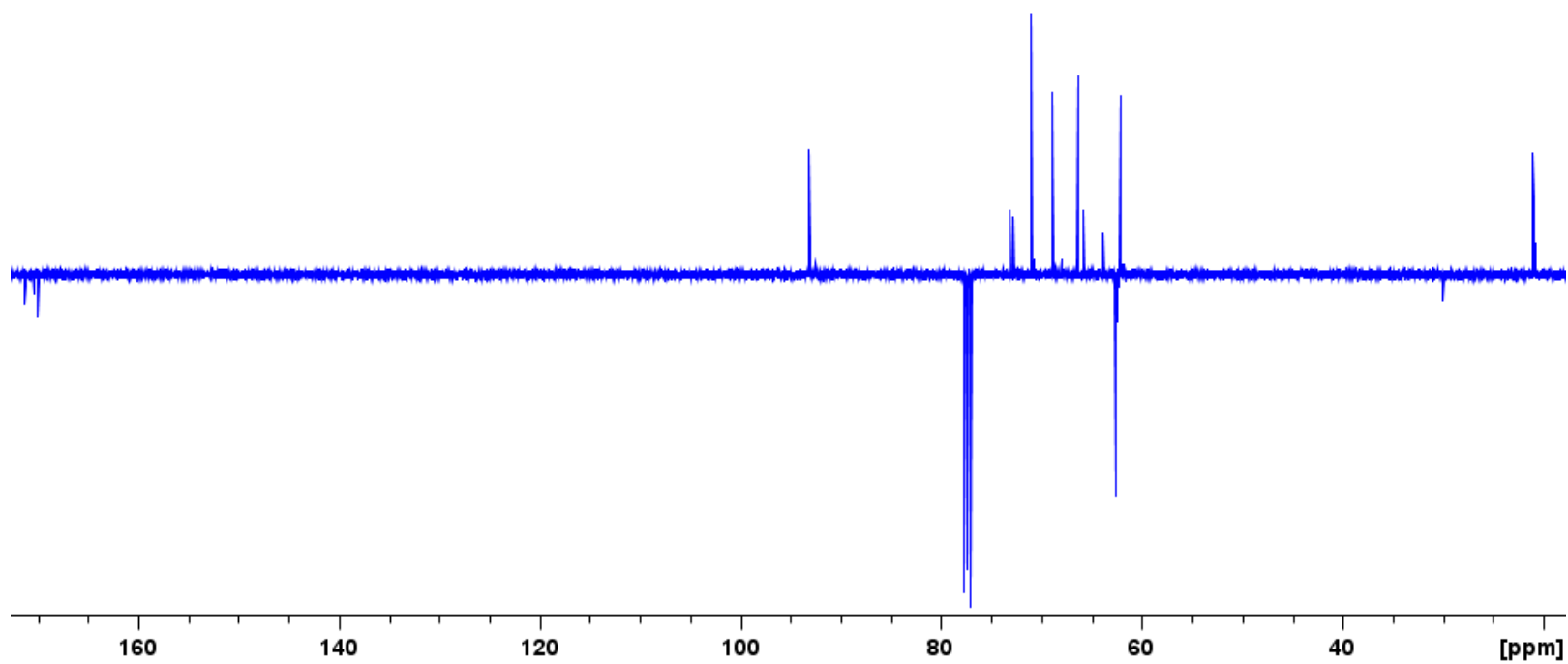
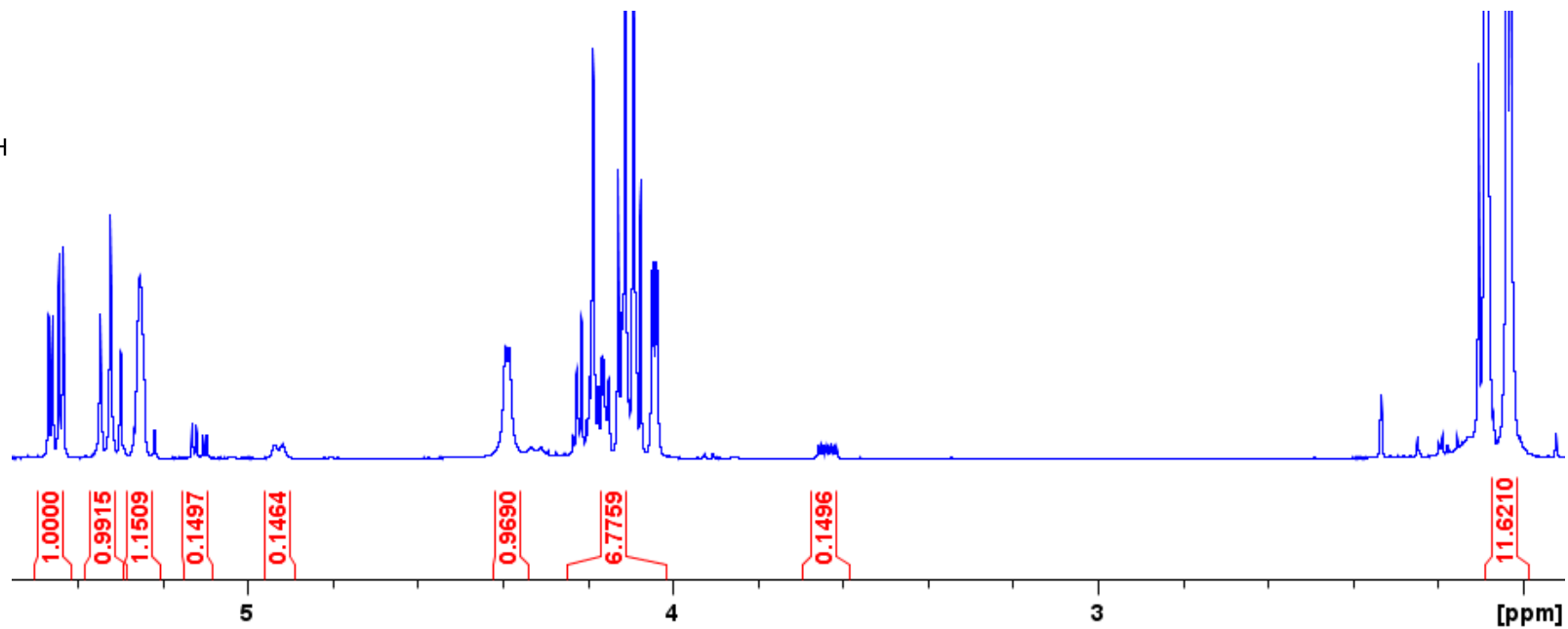
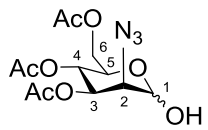
Conceptualization and methodology, A.B., F.F., S.M.-S. (lead); S.S. (supporting); investigation: L.M., S.A. and J. G.-C. (equal); M.T., L.S., A.L.R., C.E., C.V (supporting); writing of original draft: A.B., F.F., S.M.-S., S.S.

References

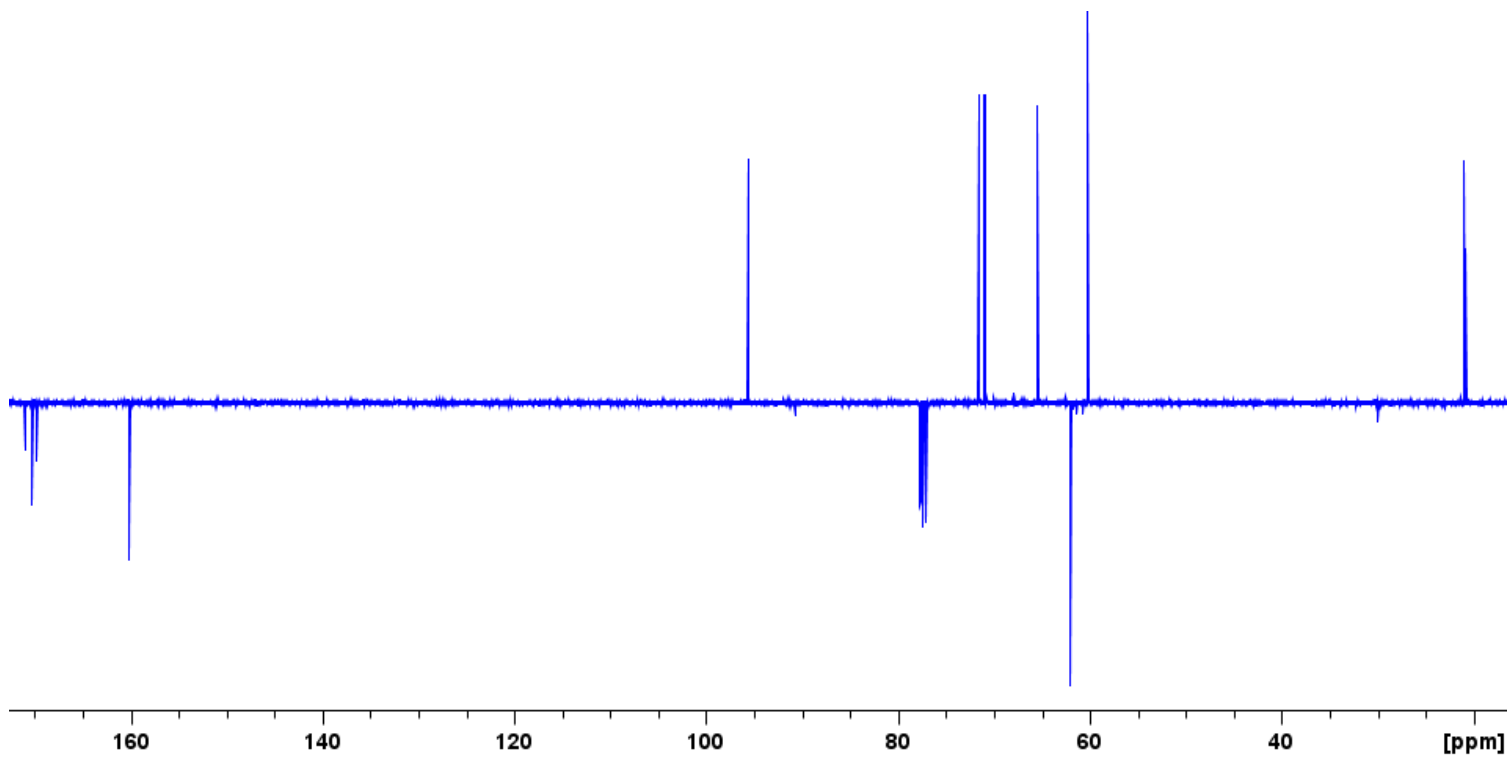
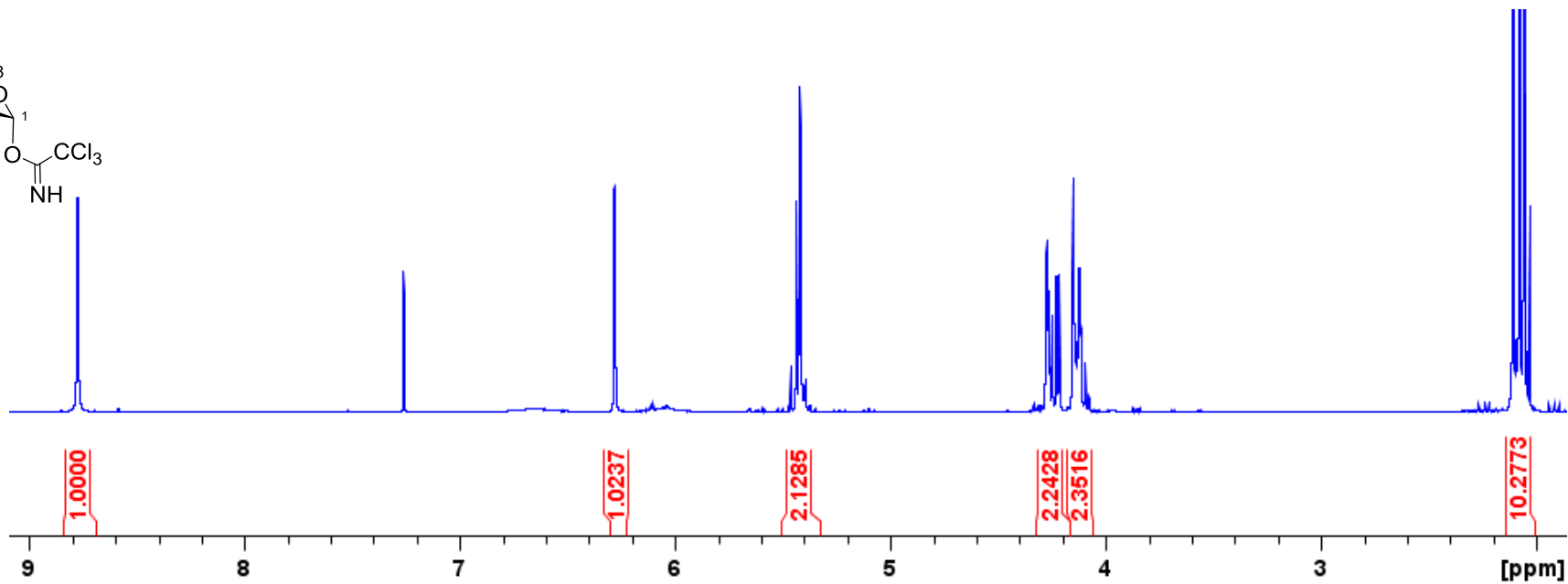
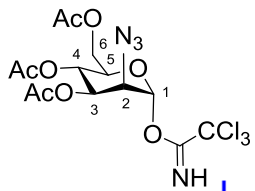
- [1] a) V. Porkolab, E. Chabrol, N. Varga, S. Ordanini, I. Sutkevičiūtė, M. Thepaut, M. J. Garcia-Jimenez, E. Girard, P. M. Nieto, A. Bernardi, F. Fieschi, *ACS Chem. Biol.* **2018**, *13*, 600-608; b) N. Varga, I. Sutkevičiūtė, C. Guzzi, J. McGeagh, I. Petit-Haertlein, S. Gugliotta, J. Weiser, J. Angulo, F. Fieschi, A. Bernardi, *Chem. Eur. J.* **2013**, *19*, 4786-4797.
- [2] J. Aretz, H. Baukmann, E. Shanina, J. Hanske, R. Wawrzinek, V. A. Zapol'skii, P. H. Seeberger, D. E. Kaufmann, C. Rademacher, *Angew. Chem. Int. Ed.* **2017**, *56*, 7292-7296.
- [3] www.rcsb.org, last accesses 20th February 2019
- [4] <https://www.schrodinger.com/protein-preparation-wizard>
- [5] Schrödinger Release 2015-4: Epik, v., Schrödinger, LLC, New York, NY, 2015.
- [6] <https://www.maybridge.com>
- [7] Schrödinger Release 2015-4: LigPrep, v., Schrödinger, LLC, New York, NY, 2015.
- [8] <https://www.schrodinger.com/glide>
- [9] Frisch, M. J.; Trucks, G. W.; Schlegel, H. B.; Scuseria, G. E.; Robb, M. A.; Cheeseman, J. R.; Scalmani, G.; Barone, V.; Petersson, G. A.; Nakatsuji, H.; Li, X.; Caricato, M.; Marenich, A. V.; Bloino, J.; Janesko, B. G.; Gomperts, R.; Mennucci, B.; Hratchian, H. P.; Ortiz, J. V.; Izmaylov, A. F.; Sonnenberg, J. L.; Williams, Ding, F.; Lipparini, F.; Egidi, F.; Goings, J.; Peng, B.; Petrone, A.; Henderson, T.; Ranasinghe, D.; Zakrzewski, V. G.; Gao, J.; Rega, N.; Zheng, G.; Liang, W.; Hada, M.; Ehara, M.; Toyota, K.; Fukuda, R.; Hasegawa, J.; Ishida, M.; Nakajima, T.; Honda, Y.; Kitao, O.; Nakai, H.; Vreven, T.; Throssell, K.; Montgomery Jr., J. A.; Peralta, J. E.; Ogliaro, F.; Bearpark, M. J.; Heyd, J. J.; Brothers, E. N.; Kudin, K. N.; Staroverov, V. N.; Keith, T. A.; Kobayashi, R.; Normand, J.; Raghavachari, K.; Rendell, A. P.; Burant, J. C.; Iyengar, S. S.; Tomasi, J.; Cossi, M.; Millam, J. M.; Klene, M.; Adamo, C.; Cammi, R.; Ochterski, J. W.; Martin, R. L.; Morokuma, K.; Farkas, O.; Foresman, J. B.; Fox, D. J. Gaussian 16 Rev. B.01, Wallingford, CT, 2016.
- [10] Case, D. A.; Darden, T. A.; Cheatham, T. E.; Simmerling, C. L.; Wang, J.; Duke, R. E.; Luo, R.; Walker, R. C.; Zhang, W.; Merz, K. M.; Roberts, B.; Hayik, S.; Roitberg, A.; Seabra, G.; Swails, J.; Götz, A. W.; Kolossváry, I.; Wong, K. F.; Paesani, F.; Vanicek, J.; Wolf, R. M.; Liu, J.; Wu, X.; Brozell, S. R.; Steinbrecher, T.; Gohlke, H.; Cai, Q.; Ye, X.; Wang, J.; Hsieh, M.-J.; Cui, G.; Roe, D. R.; Mathews, D. H.; Seetin, M. G.; Salomon-Ferrer, R.; Sagui, C.; Babin, V.; Luchko, T.; Gusarov, S.; Kovalenko, A.; Kollman, P. A. AMBER 14, University of California, San Francisco., 2014.
- [11] J. Wang, R. M. Wolf, J. W. Caldwell, P. A. Kollman, D. A. Case, *J Comput Chem* **2004**, *25*, 1157-1174.
- [12] G. M. Morris, R. Huey, W. Lindstrom, M. F. Sanner, R. K. Belew, D. S. Goodsell, A. J. Olson, *J. Comput. Chem.* **2009**, *30*, 2785-2791.
- [13] W. C. Still, M. Kahn, A. Mitra, *J. Org. Chem.* **1978**, *43*, 2923-2925.
- [14] F. Messina, M. Botta, F. Corelli, M. P. Schneider, F. Fazio, *J. Org. Chem.* **1999**, *64*, 3767-3769.
- [15] E.-H. Ryu, Y. Zhao, *Org. Lett.* **2005**, *7*, 1035-1037.
- [16] L. Medve, S. Achilli, S. Serna, F. Zuccotto, N. Varga, M. Thépaut, M. Civera, C. Vivès, F. Fieschi, N. Reichardt, A. Bernardi, *Chem. Eur. J.* **2018**, *24*, 14448-14460.

8

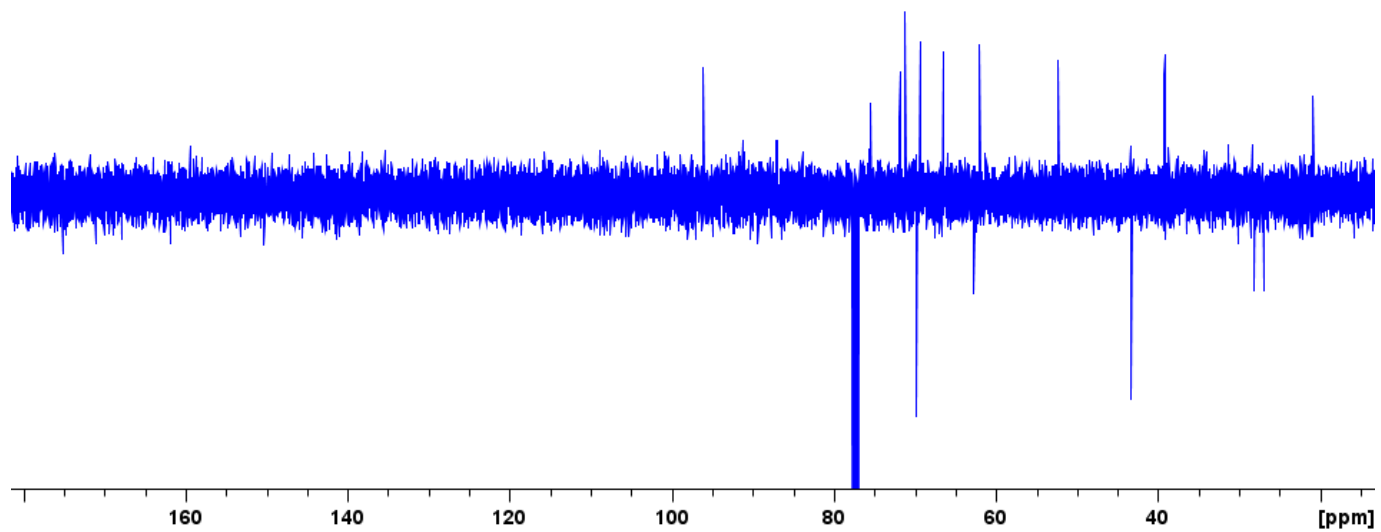
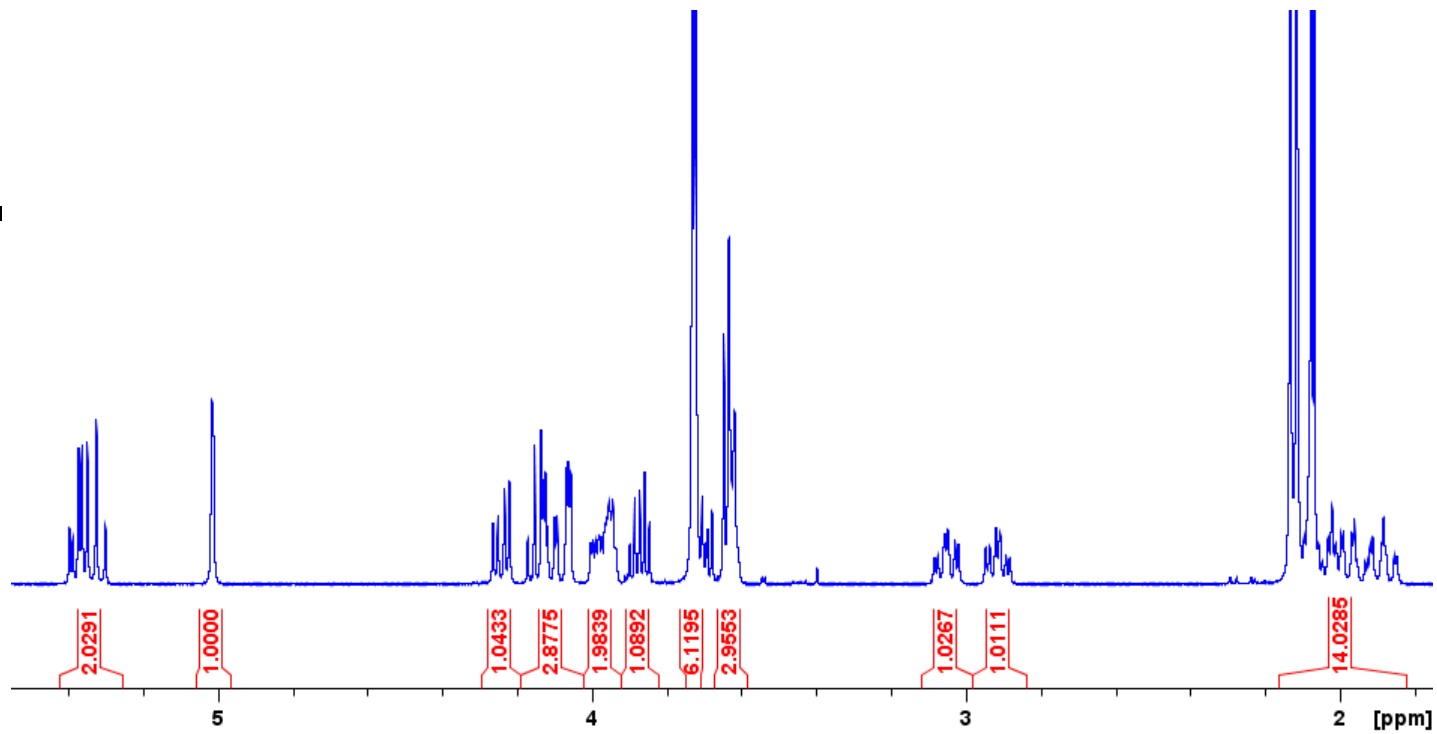
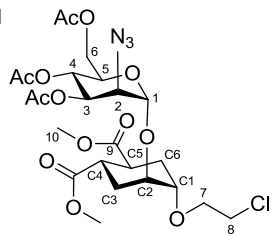




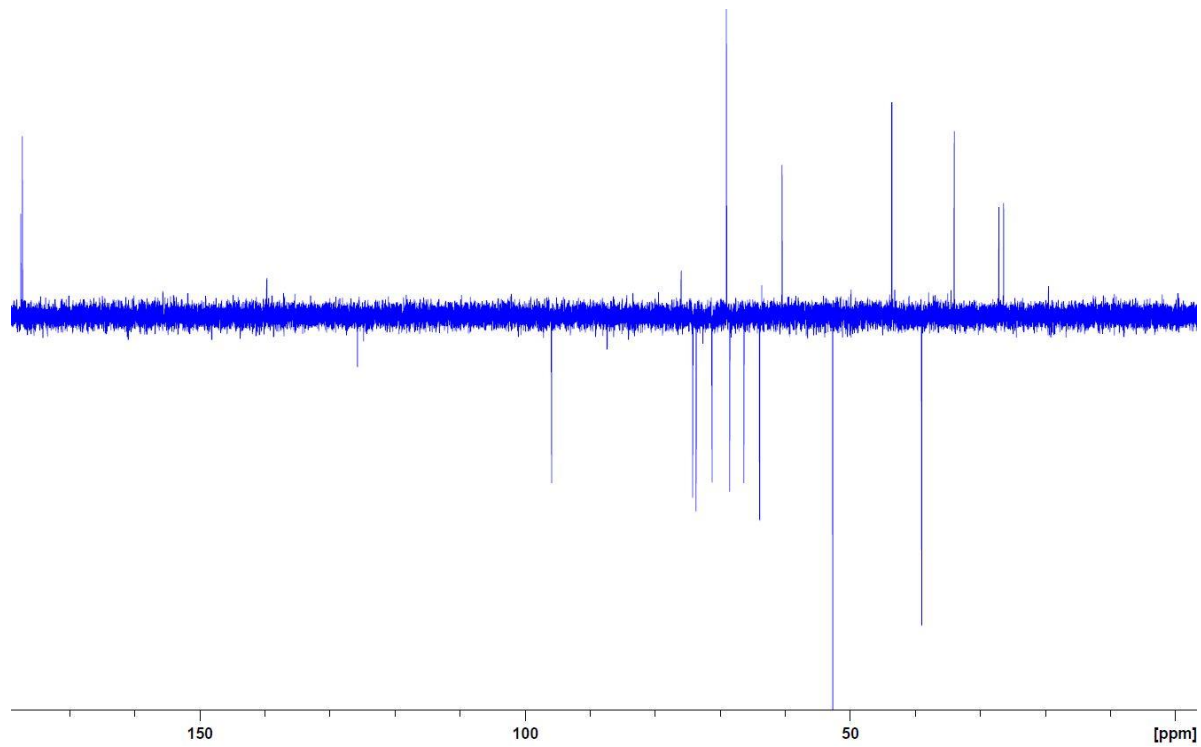
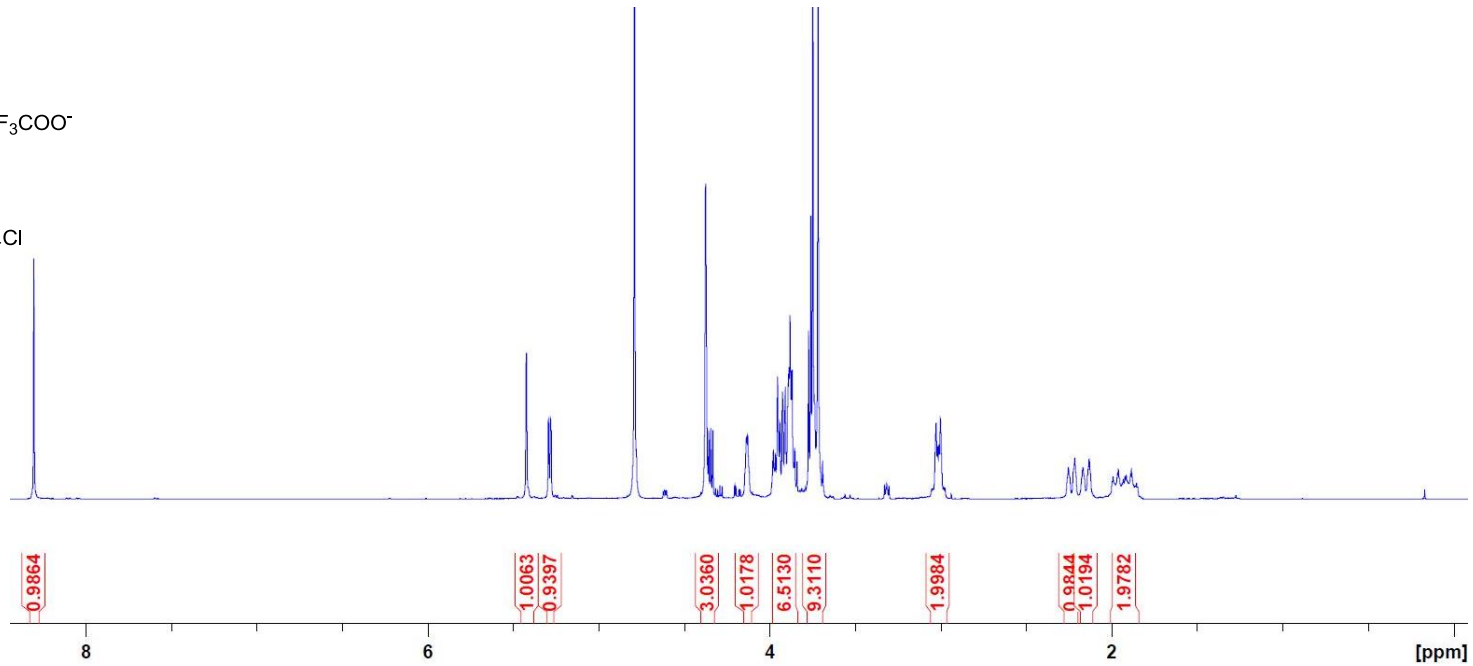
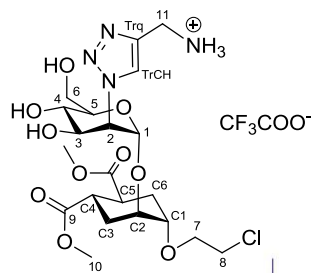
6



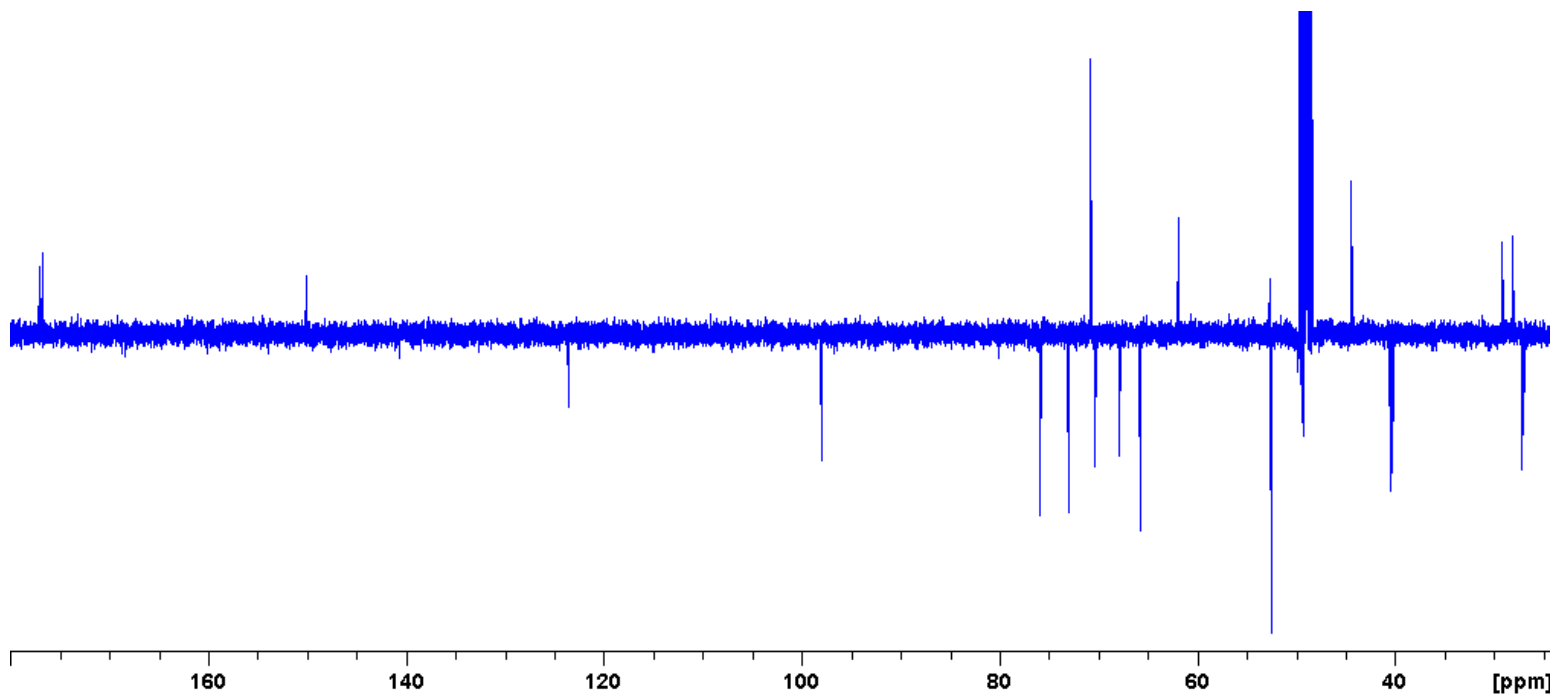
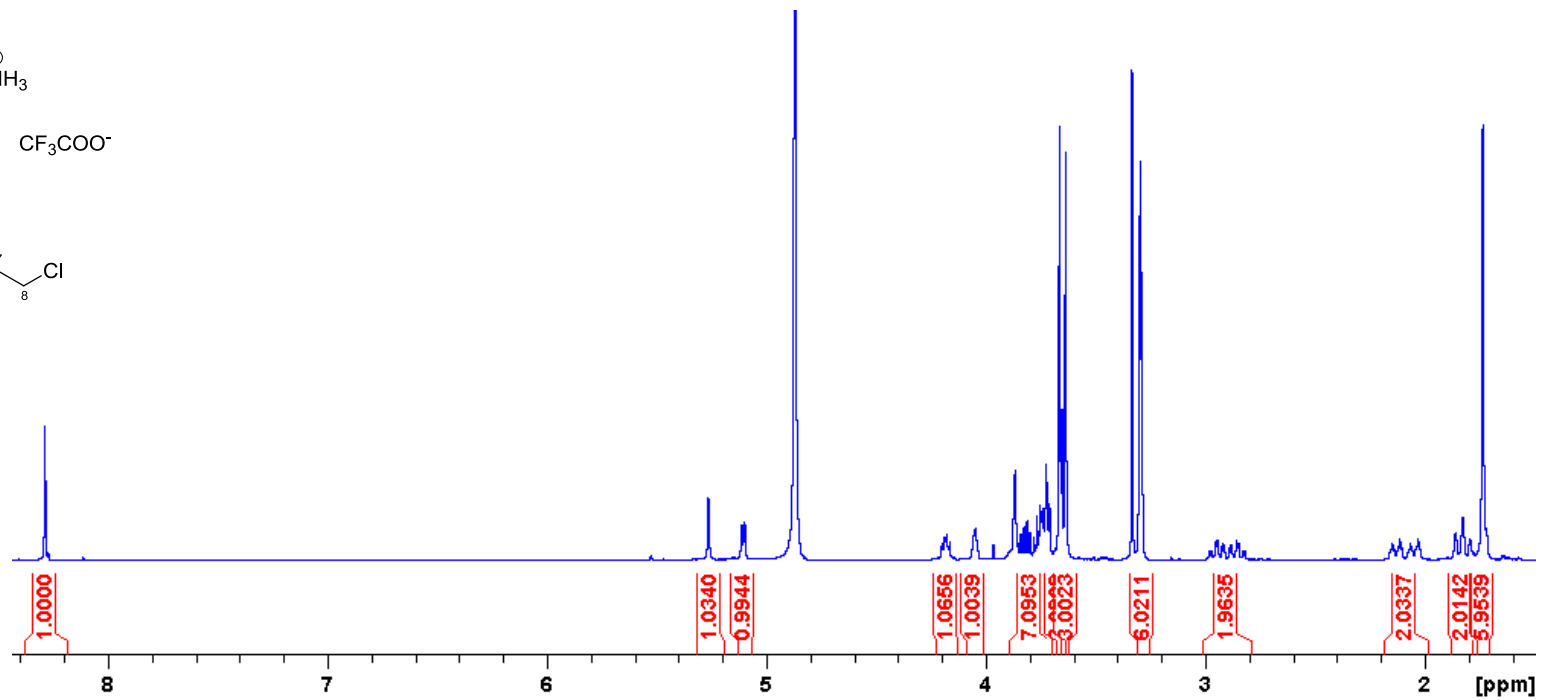
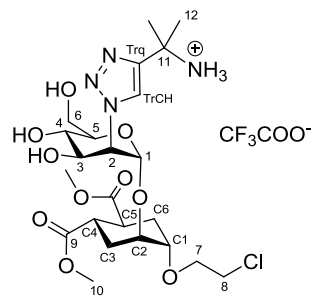
11



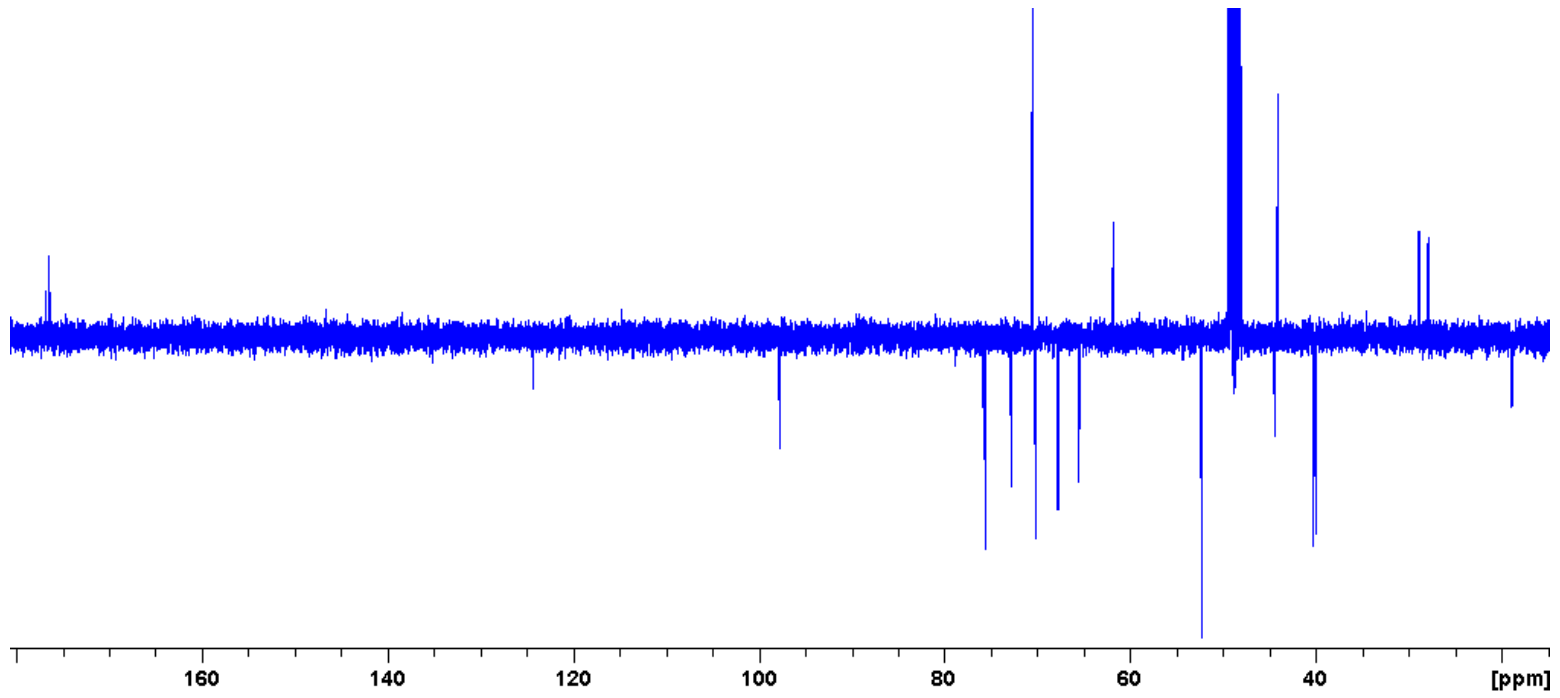
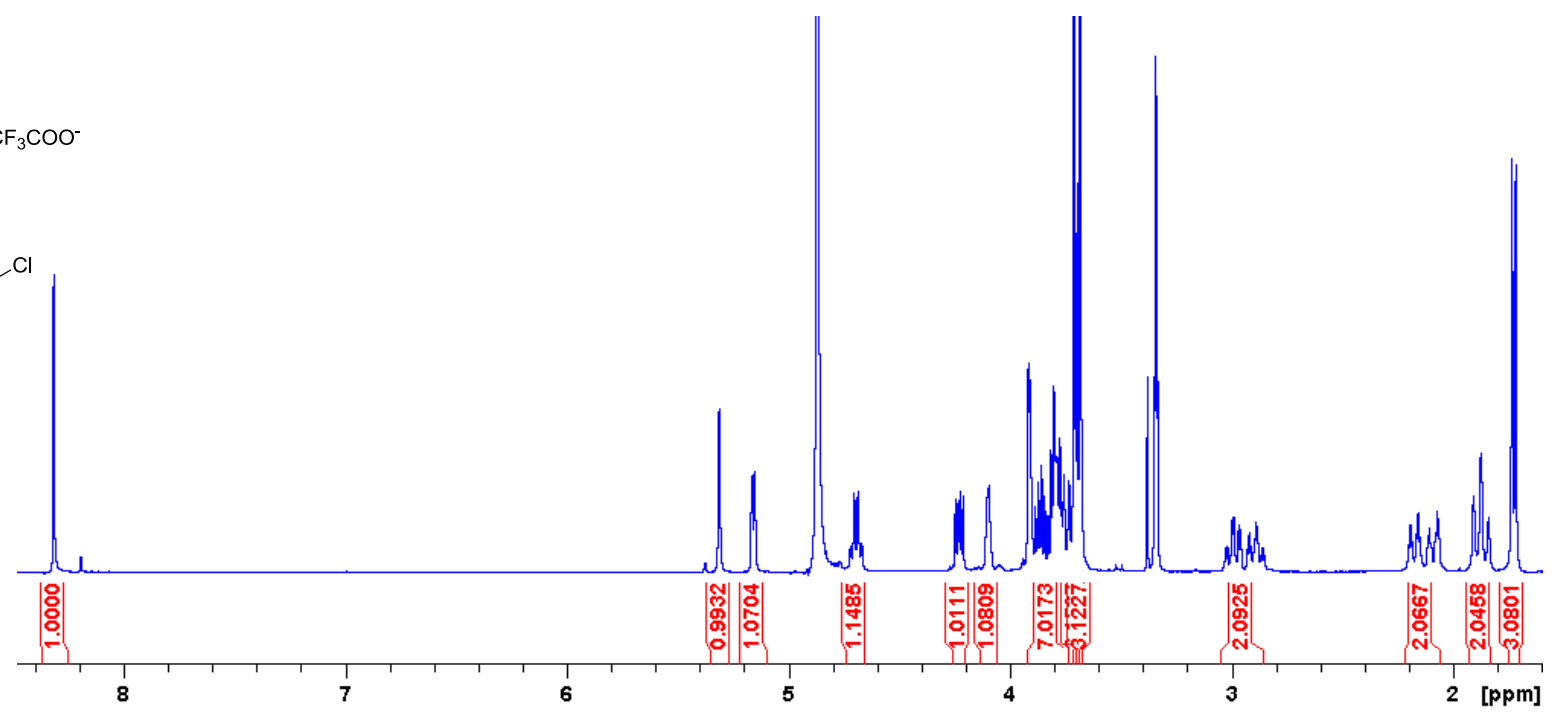
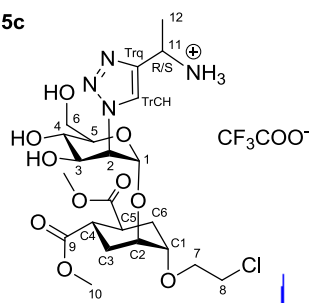
5a



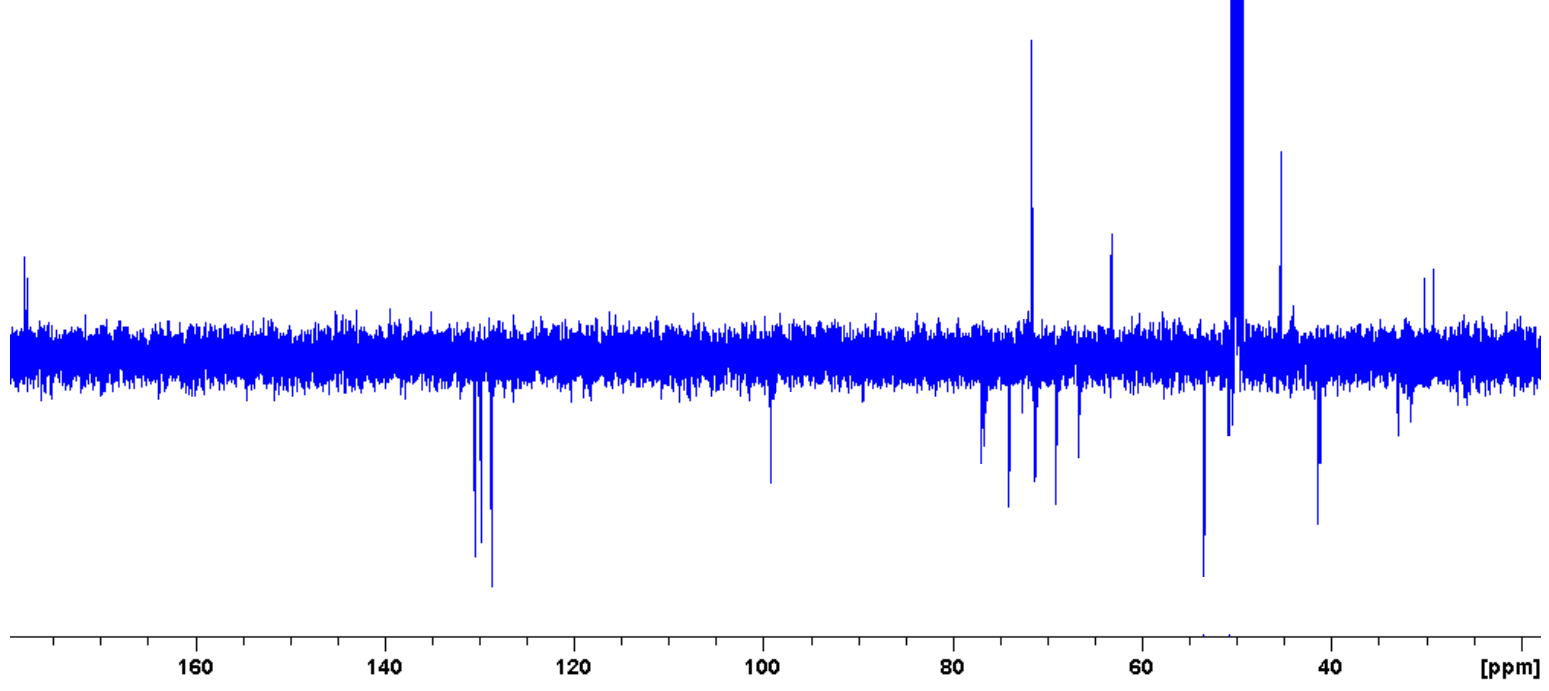
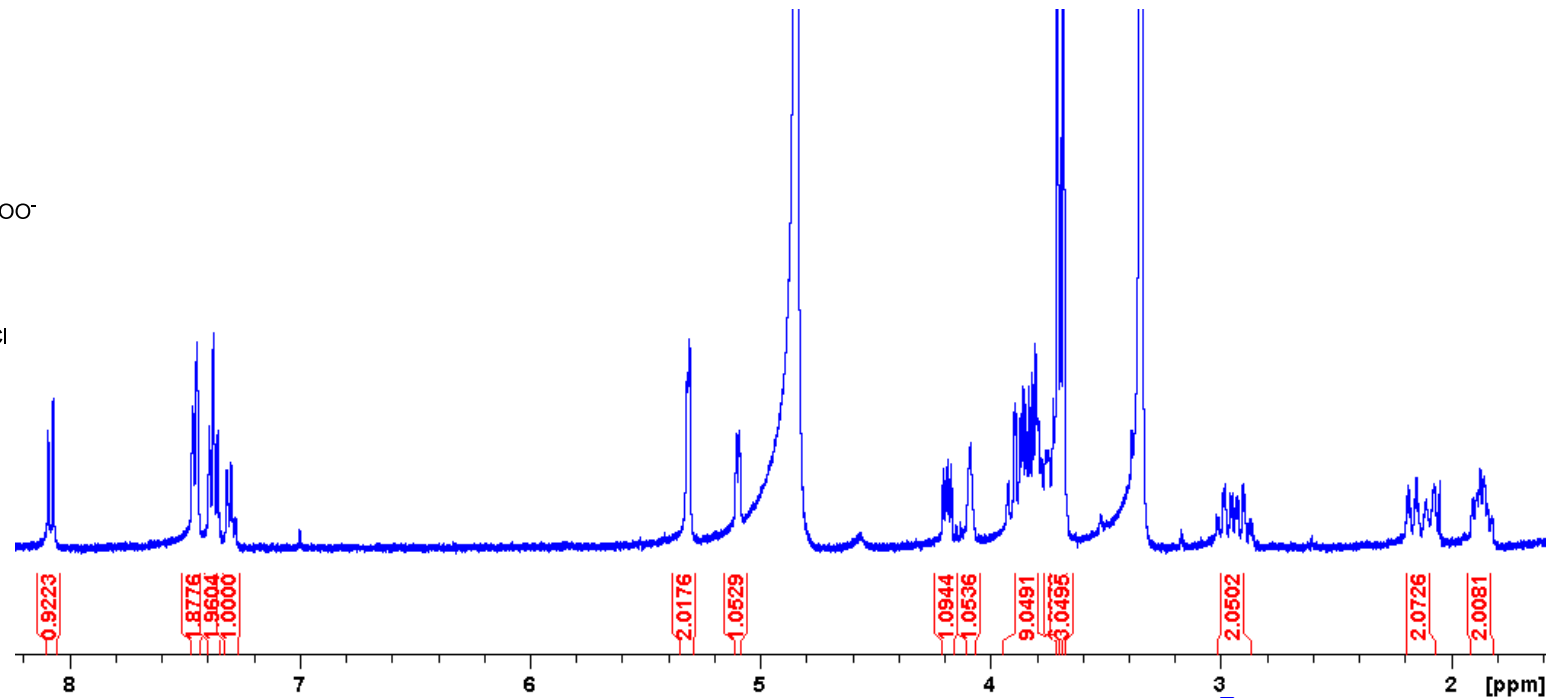
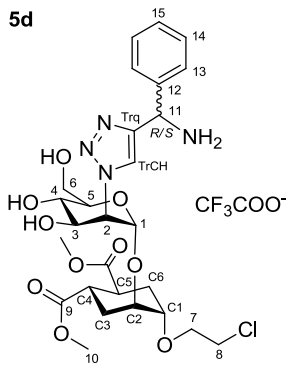
5b



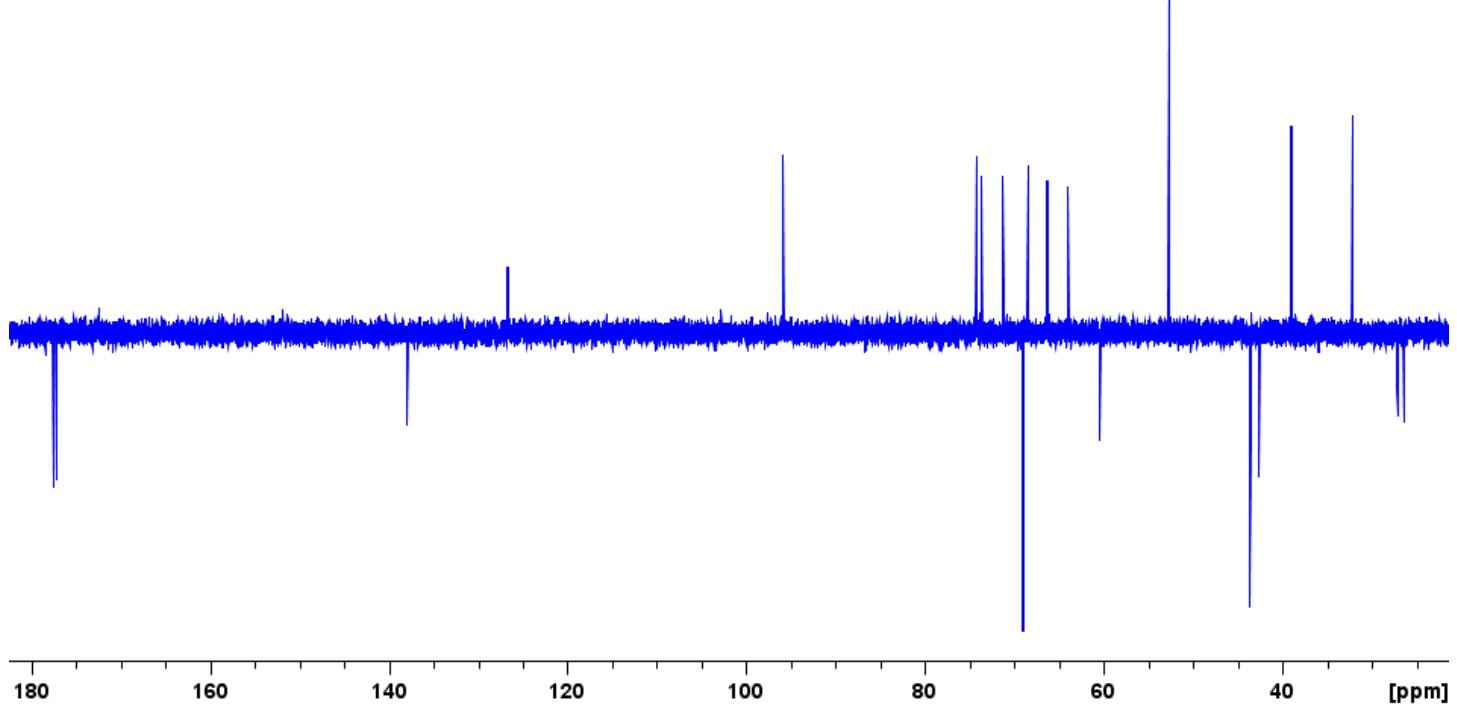
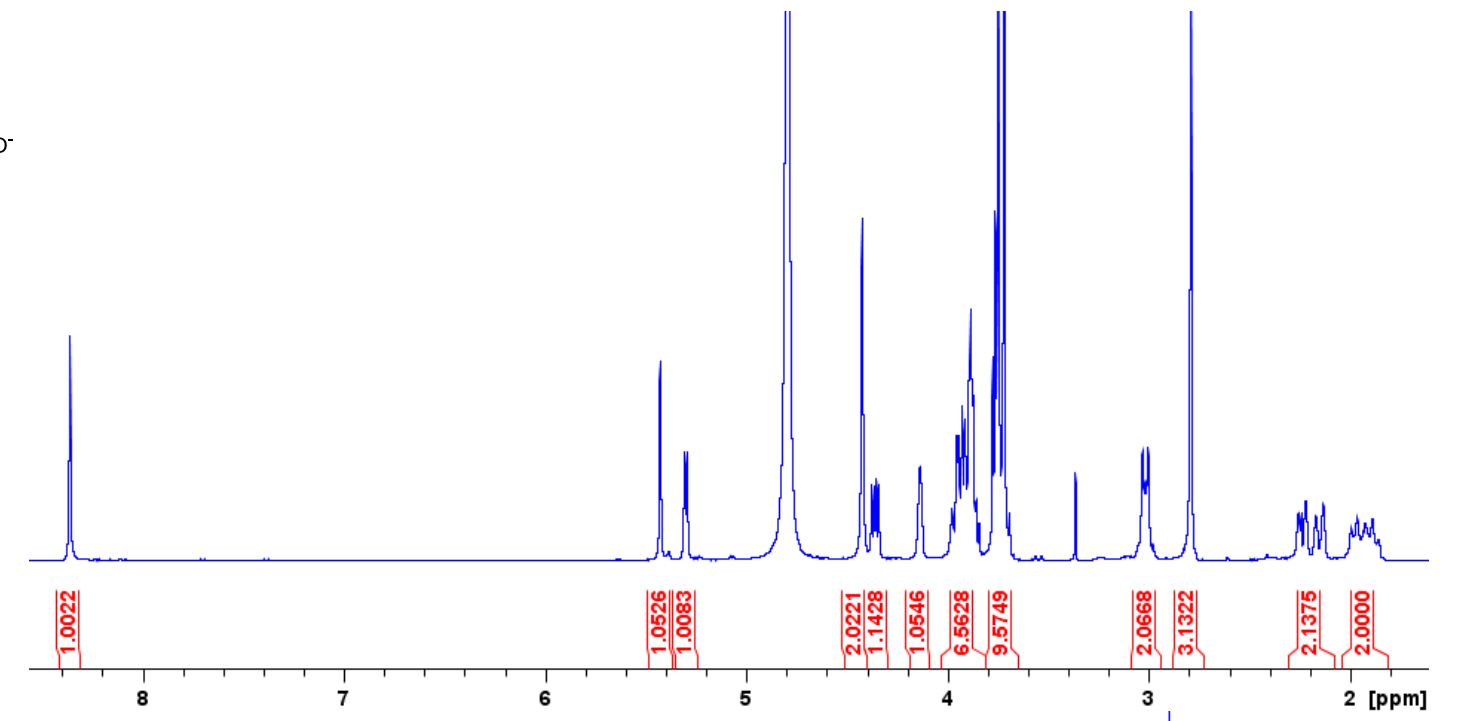
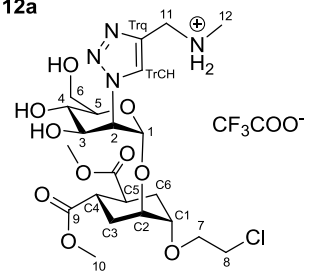
5c



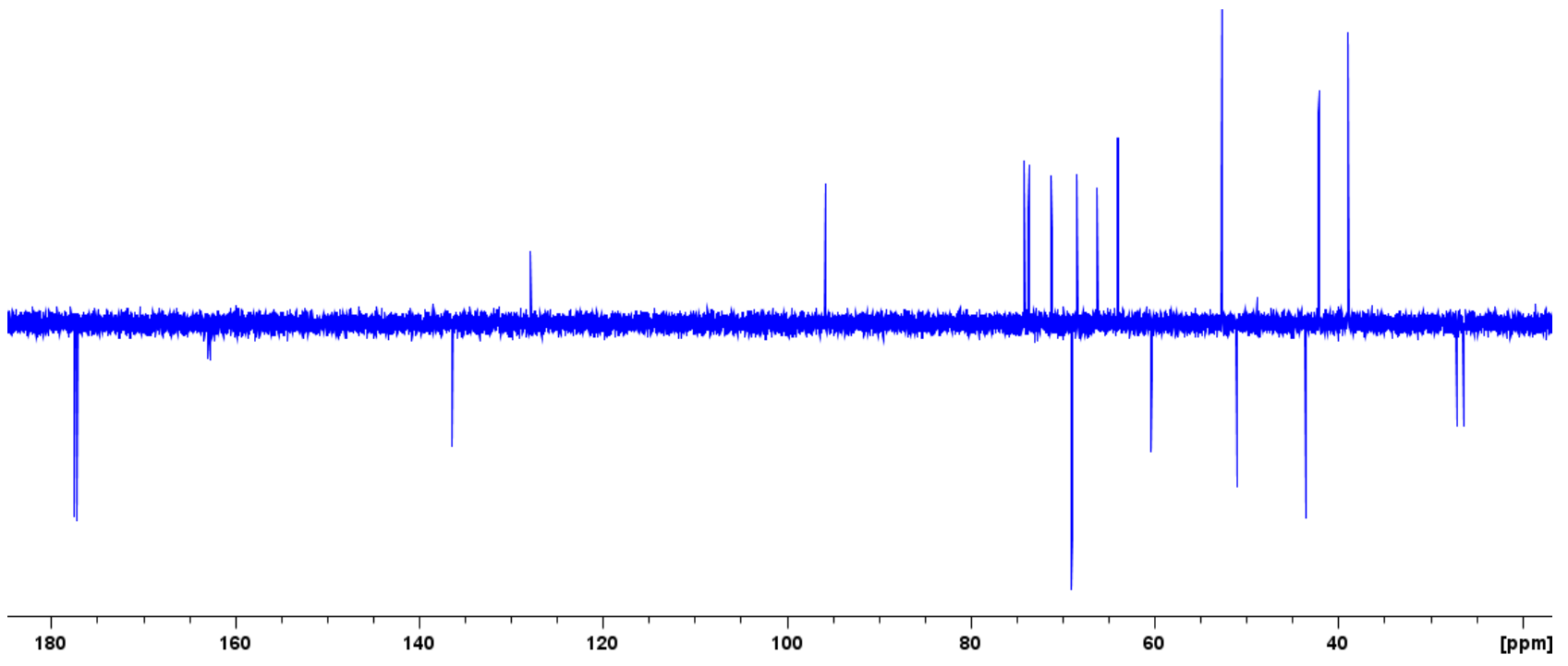
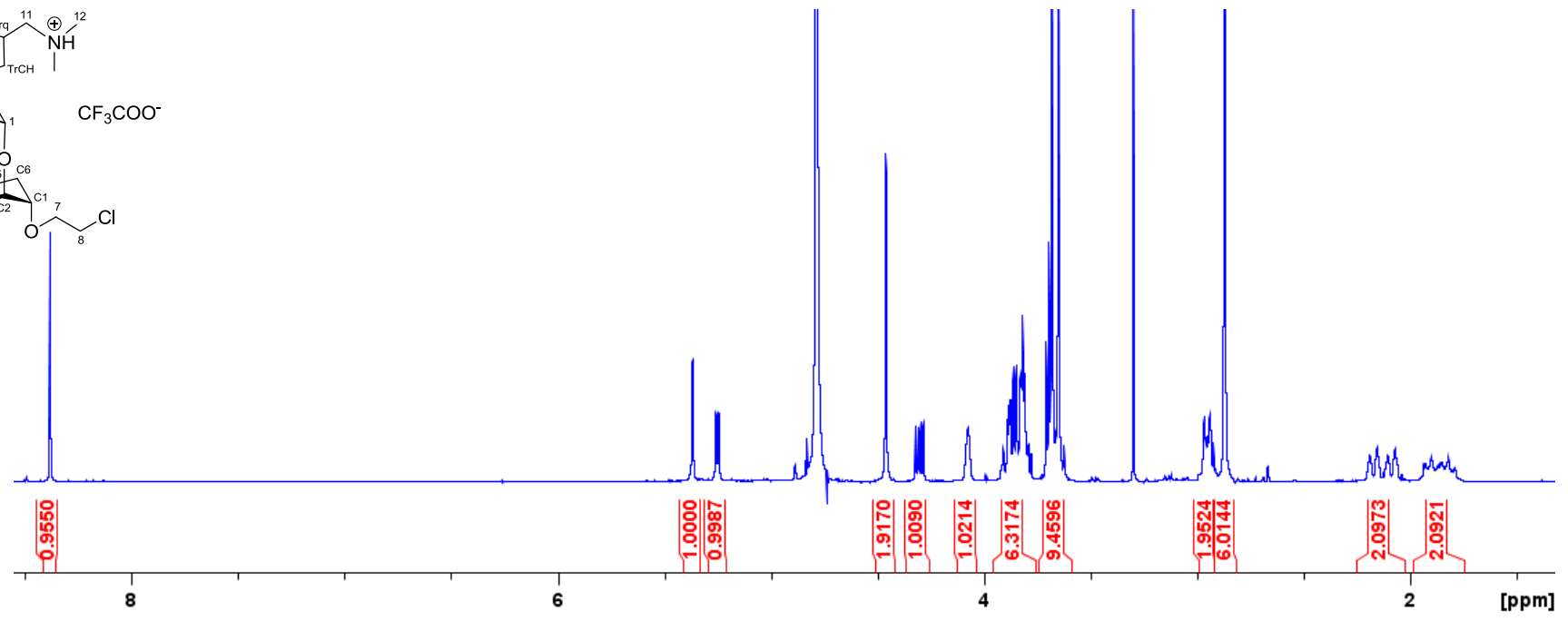
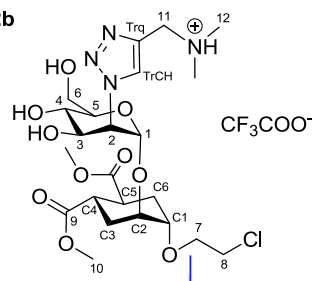
5d



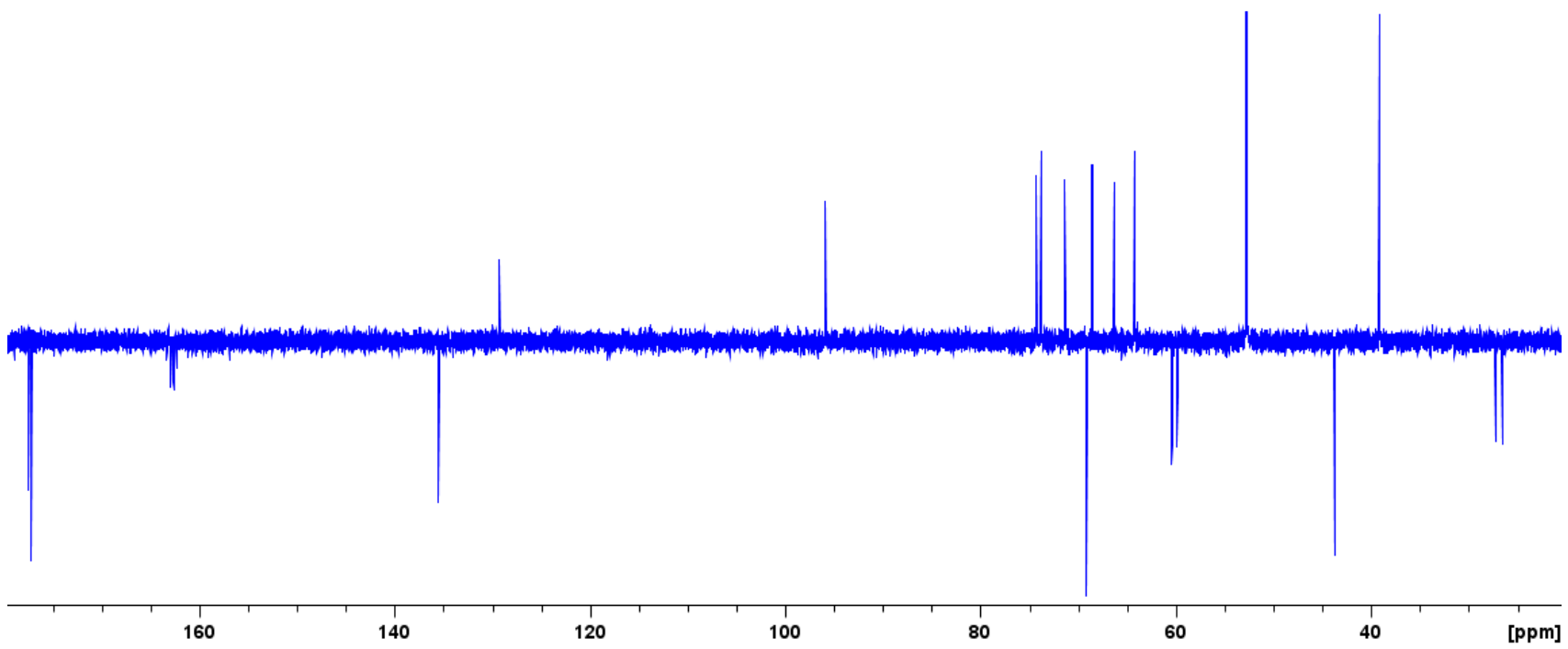
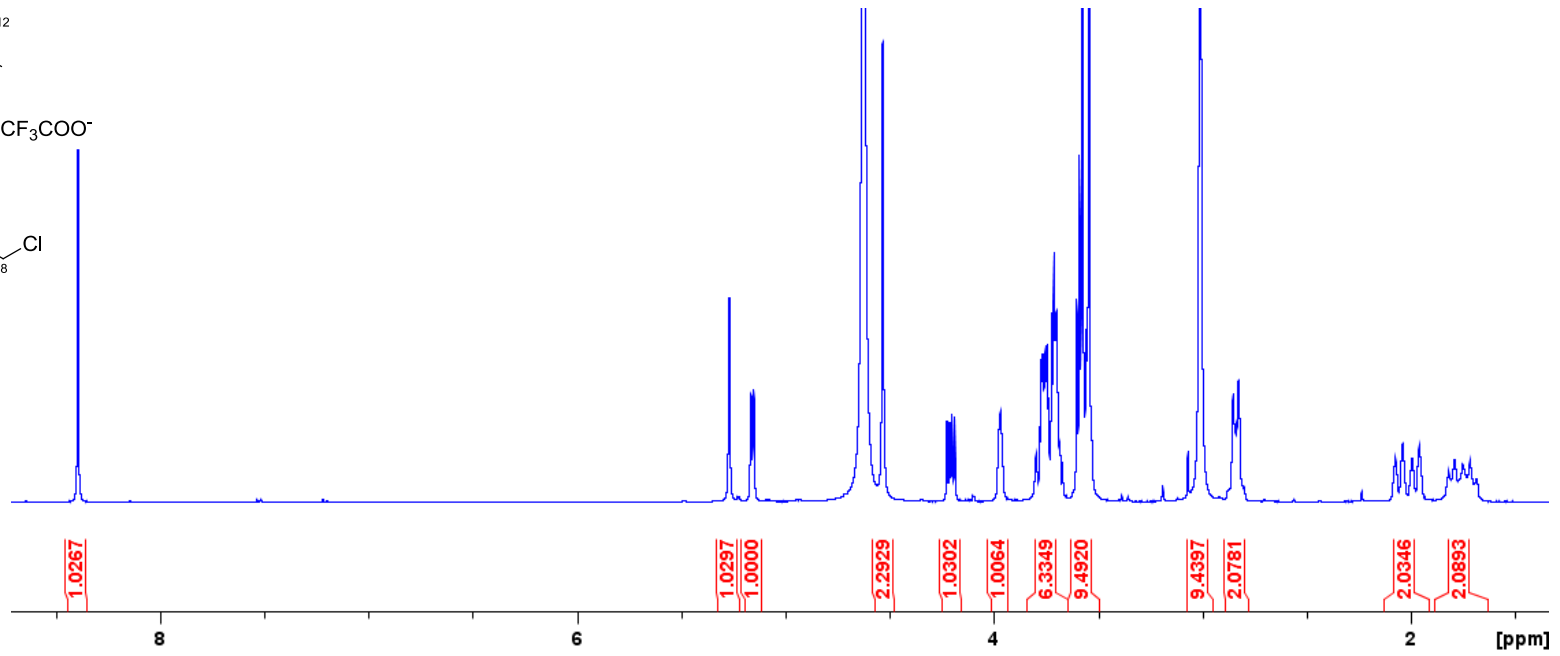
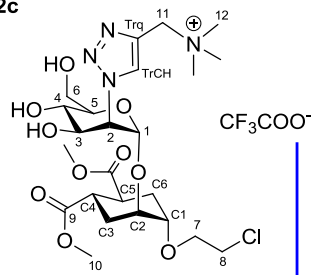
12a

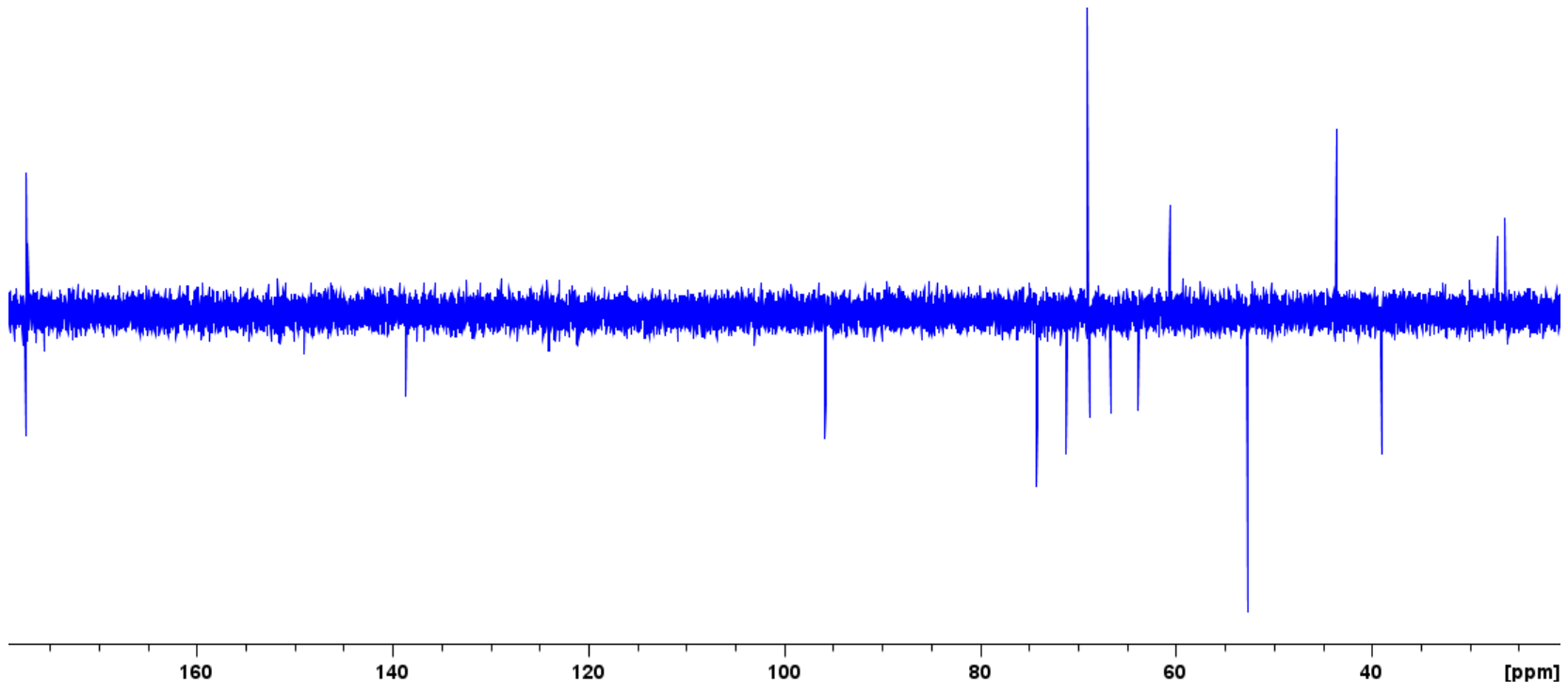
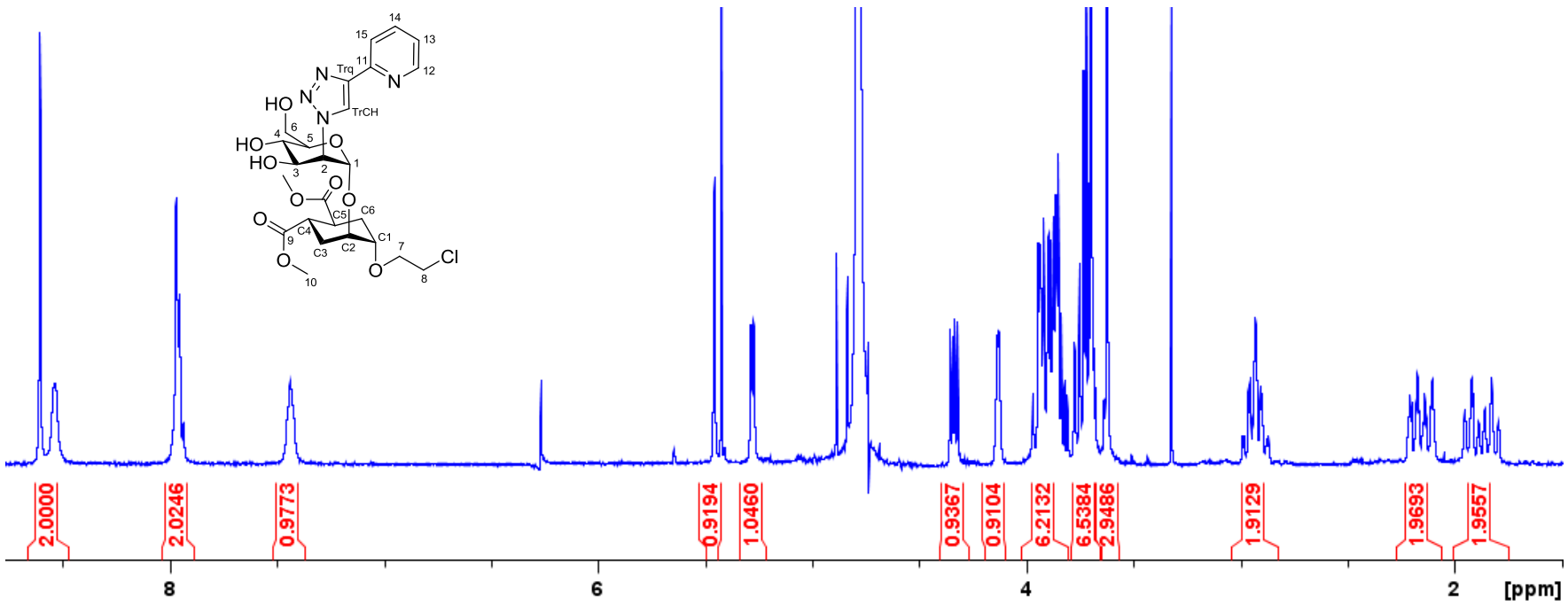


12b

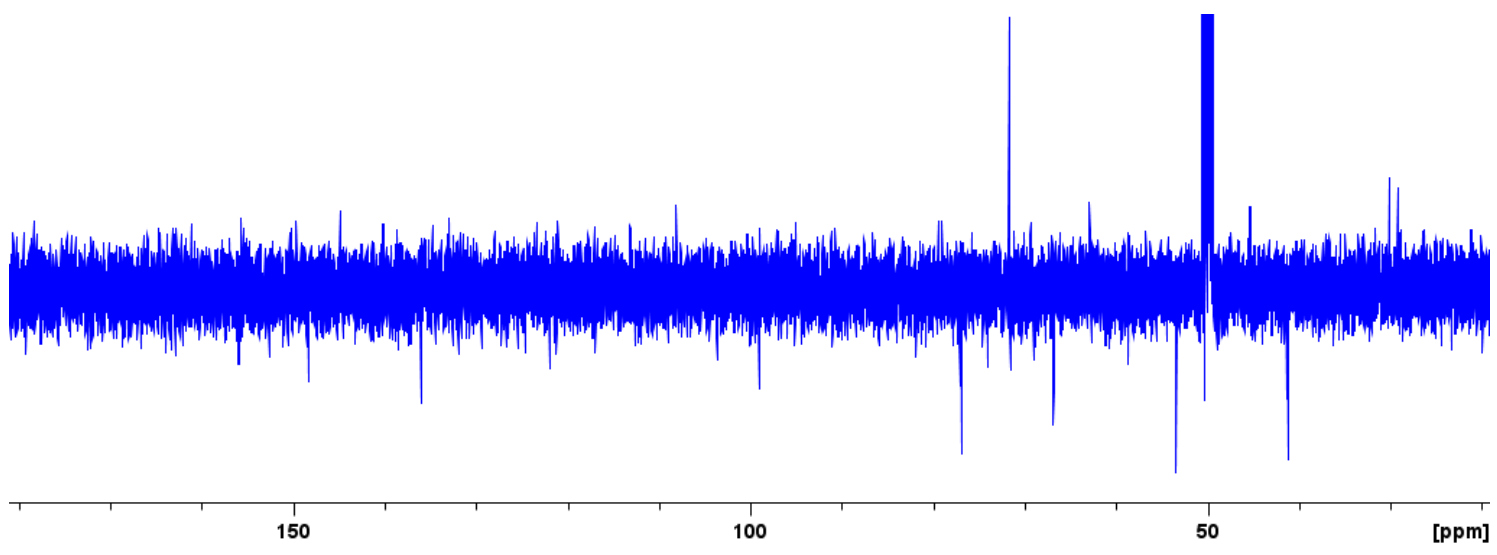
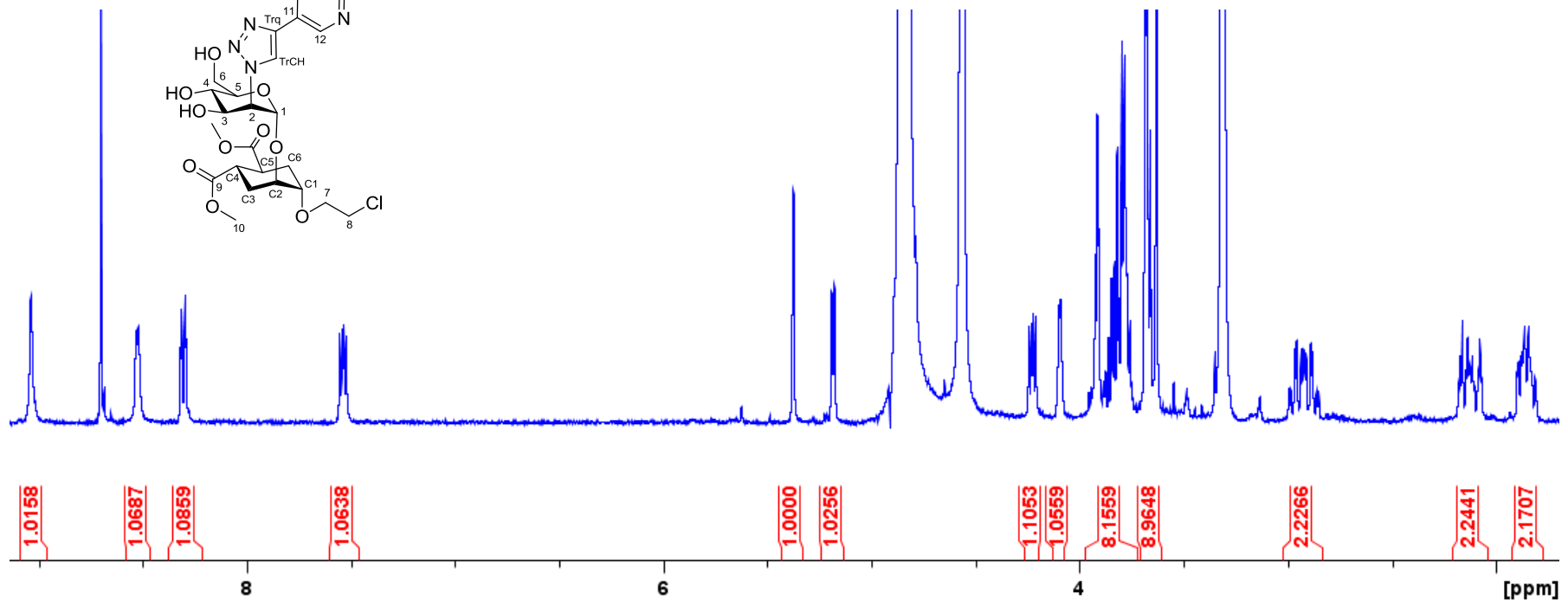
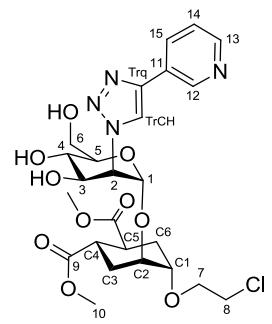


12c

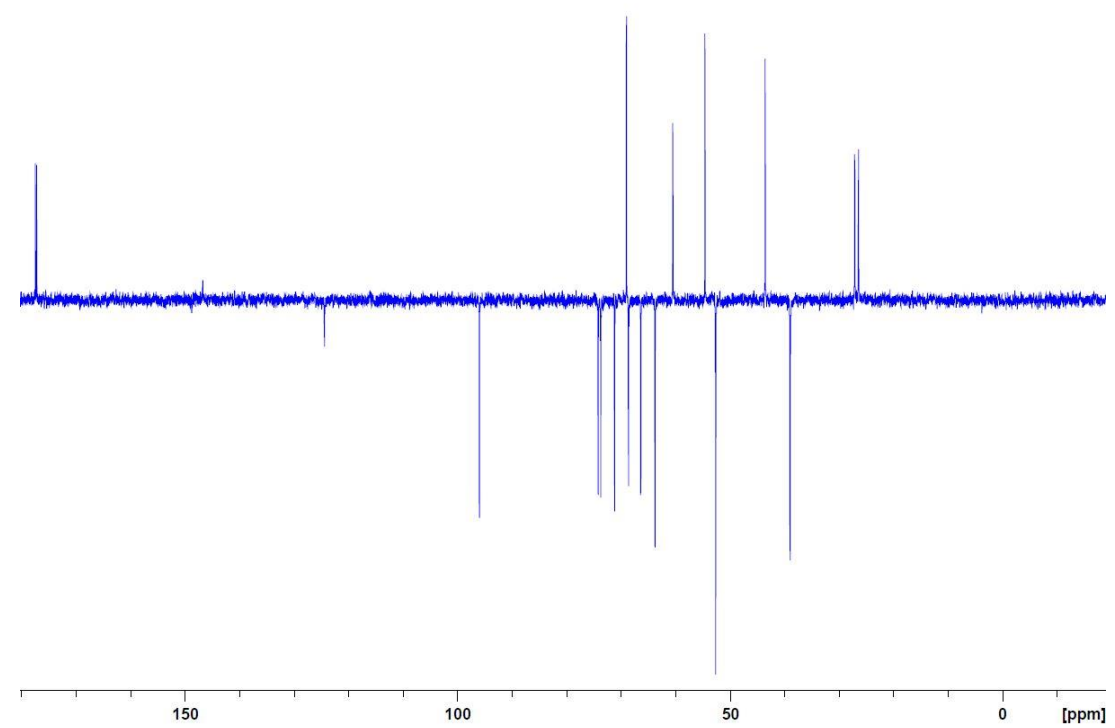
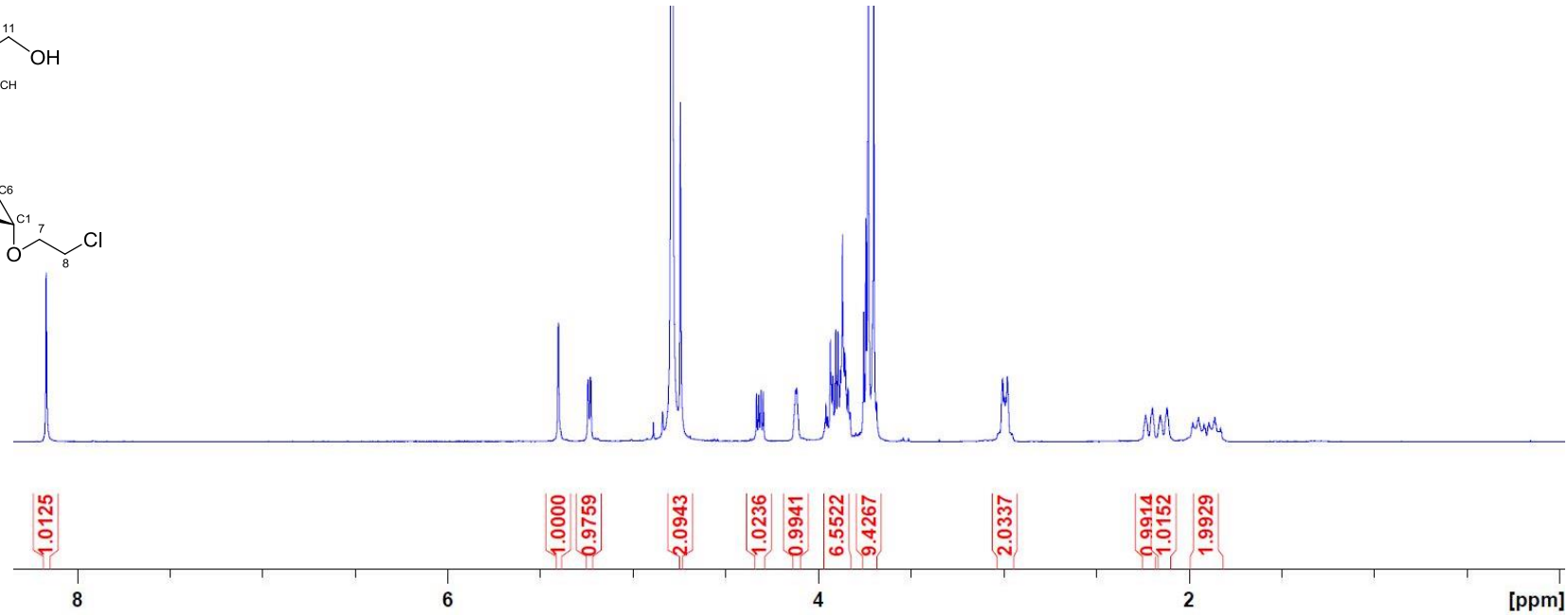
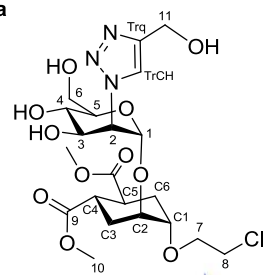




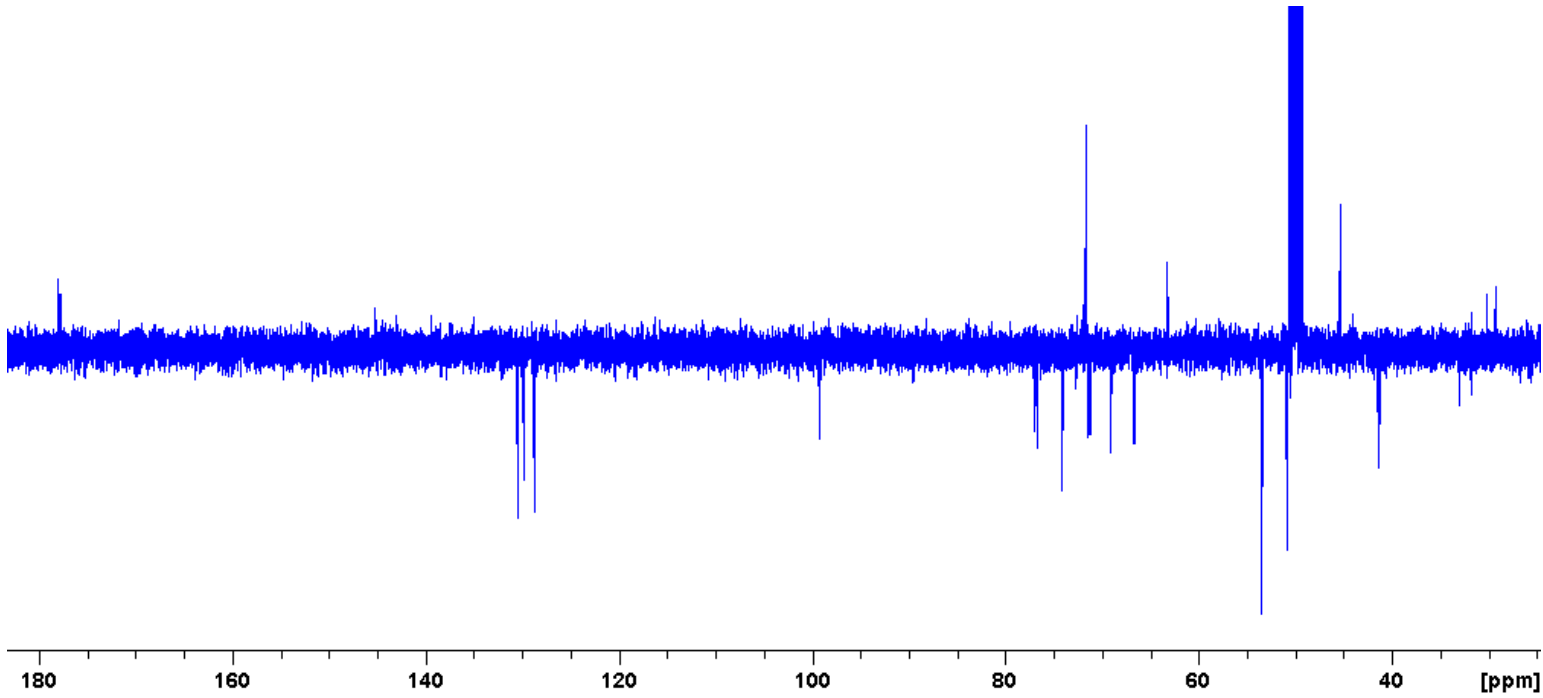
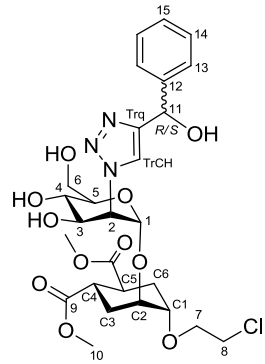
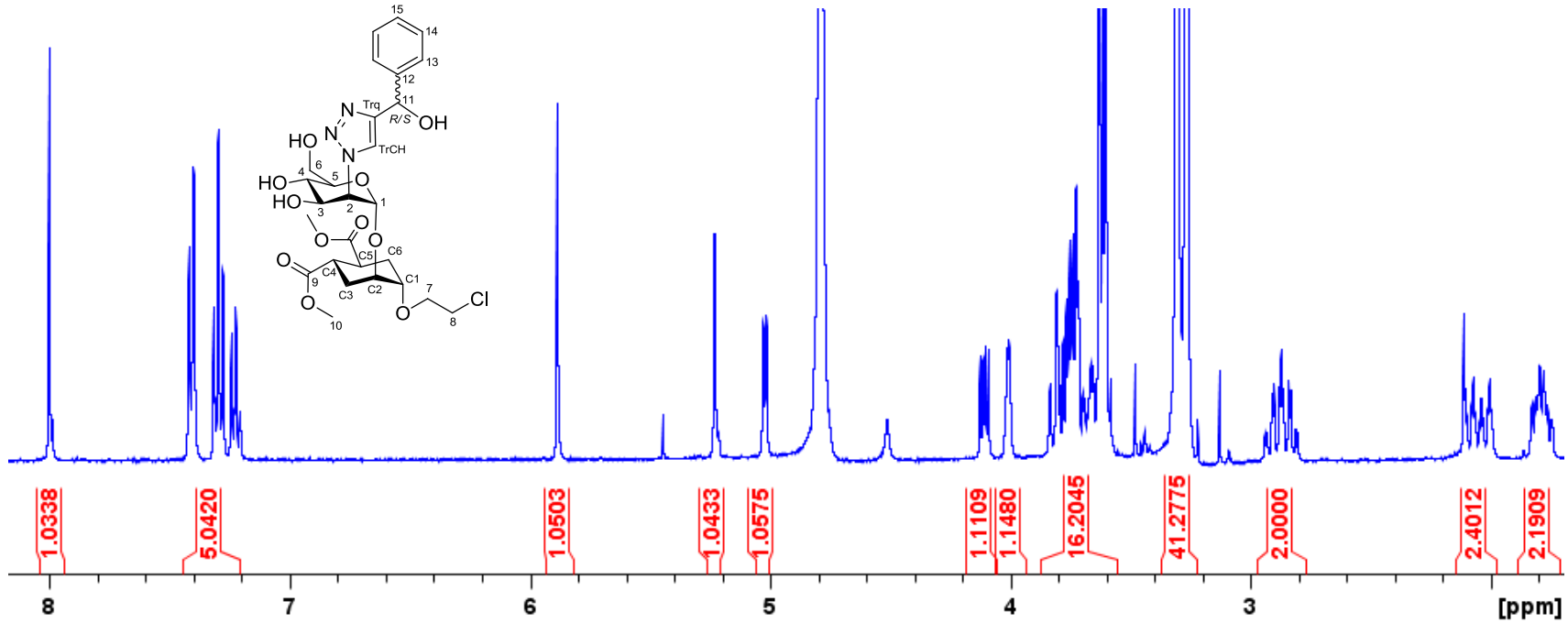
1
4



15a



15b R and S



16

